Paired box 6 programs essential exocytotic genes in the regulation of glucose-stimulated insulin secretion and glucose homeostasis

Authors: Wing Yan So[1,2], Wai Nam Liu[2], Adrian Kee Keong Teo[2,3], Guy A. Rutter[4] and Weiping Han[1,2,5*]

Affiliations:

[1]Singapore Bioimaging Consortium, Agency for Science Technology and Research (A*STAR), Singapore 138667, Singapore.

[2]Institute of Molecular and Cell Biology, A*STAR, Singapore 138673, Singapore.

[3]Department of Biochemistry and Department of Medicine, Yong Loo Lin School of Medicine, National University of Singapore, Singapore 117596, Singapore.

[4]Section of Cell Biology and Functional Genomics, Division of Diabetes, Endocrinology, and Metabolism, Imperial College London, United Kingdom.

[5]Center for Neuro-Metabolism and Regeneration Research, Guangzhou Regenerative Medicine and Health Guangdong Laboratory, Guangzhou, China

*To whom correspondence should be addressed: wh10@cornell.edu

Running title: PAX6 replenishment improves glucose-stimulated insulin secretion and glucose homeostasis

Keywords: AAV, beta-cell, cAMP, CREB, exocytosis, insulin secretion, islet, Munc18, Paired box 6, type 2 diabetes.

Abstract

The Paired box 6 (PAX6) transcription factor is crucial for normal pancreatic islet development and function. Heterozygous mutations of *PAX6* are associated with impaired insulin secretion and early-onset diabetes mellitus in human. Yet the molecular mechanism of PAX6 in controlling insulin secretion in human beta-cells and its pathophysiological role in Type 2 diabetes (T2D) remain ambiguous. We investigated the molecular pathway of PAX6 in the regulation of insulin secretion and the potential therapeutic value of PAX6 in T2D by using human pancreatic beta-cell line EndoC-βH1, the *db/db* mouse model and primary human islets. Through loss- and gain-of-function approaches, we uncovered a novel mechanism by which PAX6 modulates glucose-stimulated insulin secretion (GSIS) through a cAMP response element-binding protein (CREB)/Munc18-1/2 pathway. Moreover, under diabetic conditions, beta-cells and pancreatic islets displayed dampened PAX6/CREB/Munc18-1/2 pathway activity and impaired GSIS, which were reversed by PAX6 replenishment. Notably, adeno-associated virus-mediated PAX6 overexpression in *db/db* mouse beta-cells led to a sustained alleviation of glycemic perturbation *in vivo*. Our study highlights the pathophysiological role of PAX6 in T2D-associated beta-cell dysfunction in human, and suggests clinical translation of PAX6 gene transfer in preserving and restoring beta-cell function and T2D management.

Abbreviations

AAV	Adeno-associated virus
ATF1	Activating transcription factor 1
AUC	Area under curve
CaMK	Ca^{2+}/calmodulin-dependent protein kinase
CRE	cAMP response element
CREB	cAMP response element-binding protein
CREM	cAMP response element modulator
CRTC2	CREB-regulated transcription coactivator 2
FSK	Forskolin
GIP	Glucose-dependent insulinotropic polypeptide
GLP-1	Glucagon-like peptide-1
GSIS	Glucose-stimulated insulin secretion
HGPA	High glucose and palmitic acid
IBMX	Isobutylmethylxanthine
IPGTT	Intraperitoneal glucose tolerance test
IRS-2	Insulin receptor substrate-2
ITT	Insulin tolerance test
KSIS	Potassium-stimulated insulin secretion
PAX6	Paired box 6
PKA	Protein kinase A
shRNA	Short hairpin RNA
SM proteins	Sec1/Munc18 (SM) proteins
SNAP25	Synaptosomal-associated membrane protein 25 kDa
SNARE	Soluble *N*-ethylmaleimide-sensitive factor attachment protein receptor
STX1	Syntaxin-1
SYB2	Synaptobrevin 2
T2D	Type 2 diabetes

Introduction

Type 2 diabetes (T2D), the predominant form of diabetes, remains one of the leading causes of mortality and morbidity worldwide. T2D develops when insulin secretion is defective to compensate for the increased insulin demand elicited by insulin resistance. Physiologic and genetic data suggest that pancreatic beta-cell failure is the central event leading to the progression of insulin resistance to hyperglycemia and overt diabetes (*1, 2*). Thus, great efforts have been dedicated to the protection of beta-cells from dysfunction and death in T2D research as the pathological pathways driving beta-cell failure remain poorly characterized.

Preservation of beta-cell function and mass can be achieved by maintaining optimal expression and activity of key transcription factors that control the expression of genes essential for normal beta-cell differentiation, function and survival. Defining the roles and signaling network of these transcription factors in beta-cells provides significant insights to decipher T2D pathogenesis and more importantly to develop effective approaches for T2D management. In this regard, paired box 6 (PAX6) is a transcription factor pivotal for the normal development of pancreas. PAX6 deletion greatly reduces alpha- and beta-cell mass with dramatic increase in ghrelin expression, a gut hormone transiently expressed in fetal pancreas (*3-5*). Previous studies revealed that PAX6 is an activator of several beta-cell genes involved in insulin synthesis, glucose sensing, insulin secretion and thereby maintaining mature beta-cell function in rodents (*6, 7*). Correspondingly, PAX6 deficiency in adult murine islet cells causes progressive hyperglycemia and glucose intolerance with reduced insulin production and secretion (*5, 8, 9*). In human, clinical studies revealed that humans heterozygous for *PAX6* show glucose intolerance and early-onset diabetes associated with impaired insulin secretion (*10-12*). These observations strongly suggest the essential regulatory role of PAX6 in insulin secretion not only in rodents but also in human.

However, evidence regarding the role of PAX6 in islet function and the pathophysiology of human T2D remains fragmentary.

cAMP response element (CRE)-binding protein (CREB) has emerged as another key transcription factor modulating beta-cell proliferation and survival. Glucose is a natural activator of CREB. Upon glucose stimulation, glycolysis and mitochondrial oxidative metabolism lead to increased ATP/ADP ratio and closure of ATP-sensitive K^+ channels, followed by membrane depolarization and Ca^{2+} influx. Ca^{2+} sensors then trigger exocytosis of insulin granules (*13*). The ATP generated would be converted into cAMP by adenylyl cyclase; elevated cAMP levels enhance glucose-stimulated insulin secretion (GSIS) through protein kinase A (PKA)-dependent and -independent mechanisms (*14*). On the other hand, catalytic subunits of activated PKA would translocate to the nucleus and phosphorylate CREB at serine 133 (Ser133) (*15*). Ca^{2+} influx also promotes CREB phosphorylation by activating Ca^{2+}/calmodulin-dependent protein kinase (CaMK) IV. Phosphorylation of Ser133 is a prerequisite for CREB-mediated transcription (*16*). Activated CREB binds to a conserved CRE that was first documented as an eight-base-pair palindrome, TGACGTCA with a higher conservation at the 5' end (TGACG). The CRE also occurs as a half-site motif (TGACG/CGTCA) (*17, 18*). CREB-dependent gene regulation is essential to govern beta-cell proliferation and survival (*19, 20*). Disruption of CREB activity in beta-cells induces apoptosis, glucose intolerance and ultimately overt diabetes (*21, 22*). Whilst most of the previous studies illustrated the role of CREB signaling in beta-cell survival, however, being a transcription factor activated by a variety of insulin-secreting stimuli including glucose, incretin hormones such as glucagon-like peptide-1 (GLP-1) and glucose-dependent insulinotropic polypeptide (GIP) (*23*), the role of CREB in insulin secretion remains obscure.

Exocytosis plays a critical role in cellular processes as it is the final but common step of neurotransmission and hormone secretion. Sec1/Munc18 (SM) proteins and soluble *N*-ethylmaleimide-sensitive factor attachment protein receptor (SNARE) proteins are the two key protein families of exocytosis. Three conserved SNARE proteins including syntaxin-1 (STX1), synaptosomal-associated protein 25 (SNAP25) and synaptobrevin 2 (SYB2) are involved to promote granule exocytosis by forming a heterotrimeric complex (*24, 25*). SM proteins are essential regulators of SNARE protein-mediated vesicle docking or fusion events, acting as high affinity binding partners for syntaxin proteins (*26*). There are three plasma membrane-localized SM proteins (Munc18-1/2/3) expressed in mammalian cells which were found to play specific roles in beta-cell insulin secretion and to modulate glucose homeostasis. Depletion of Munc18-1, Munc18-2 or Munc18-3 causes defective GSIS in mouse and human islets whereas overexpression of either Munc18-1 or Munc18-2 potentiates GSIS in human islets (*27-29*). On the other hand, down-regulation of SM proteins has been observed in pancreatic islets of insulin-resistant rats and T2D patients (*28, 30, 31*), suggesting a positive association between islet Munc18 expression level and islet function in both rodents and human. While the pivotal function of these proteins in insulin secretion is irrefutable, the regulatory mechanism of SM proteins, especially their diminution during T2D remains ambiguous. Therefore, deciphering the mechanism that regulates SM protein expression or activity is of paramount importance to understand the pathophysiology of T2D, paving the way for generation of innovative anti-diabetic therapy.

In this study, we uncovered a novel mechanism by which PAX6 regulates human beta-cell insulin secretion through modulation of CREB signaling pathway, a direct transcriptional regulator of exocytotic proteins Munc18-1 and Munc18-2. Suppression of this pathway under

diabetic condition results in defective insulin secretion; while restoration of PAX6 expression rescues CREB activation and Munc18-1/2 down-regulation, enhances insulin-secreting capacity and ultimately ameliorates glucose homeostasis.

Results

PAX6 regulates Munc18-1/2 expression in human pancreatic beta-cells. Exocytosis is the final and critical step of insulin secretion. To elucidate the role of PAX6 in insulin exocytosis, the expression levels of several core exocytotic proteins were first measured under conditions with PAX6 manipulated. Lentivirus-mediated PAX6 overexpression in EndoC-βH1 cells increased mRNA levels of *MUNC18-1* and *MUNC18-2* by ~3-fold and 2-fold over the respective control levels (Fig. 1A) without altering the mRNA levels of other selected exocytotic proteins including *MUNC18-3*, *MUNC13-1*, *SNAP25*, *SYB2* and *STX1A*. Consistently, short hairpin RNA (shRNA)-mediated *PAX6* knockdown significantly decreased mRNA levels of *MUNC18-1* and *MUNC18-2* (Fig. 1B; ~50% and 70% of control group respectively) without affecting the mRNA levels of some other exocytotic proteins. In addition, we examined Munc18-1 and Munc18-2 protein expression under PAX6 overexpression and knockdown conditions which confirmed the mRNA expression findings (Fig. 1C and 1D). These results showed that PAX6 is a positive regulator of Munc18-1/2 expression and loss of PAX6 would lead to reduced expression of Munc18-1/2.

PAX6 regulates GSIS through modulation of Munc18-1/2 expression. We next investigated the role of PAX6/Munc18-1/2 axis in insulin secretion. PAX6 knockdown in EndoC-βH1 cells led to a decrement in protein levels of both Munc18-1 and Munc18-2, which were reversed by individual overexpression of either Munc18-1 or Munc18-2 without cross-affecting the other one

(Fig. S2A and S2B). Although insulin content was lower in cells with PAX6 knockdown, there was no significant difference in basal insulin secretion (Fig. 2A and S3A). However, GSIS was greatly suppressed in the PAX6 knockdown group when compared with the control group. Notably, individual overexpression of Munc18-1 or Munc18-2 did not exert significant effect on GSIS, but mitigated the defective GSIS caused by PAX6 knockdown (Fig. 2A). Perifusion of EndoC-βH1 cells with high glucose resulted in a burst of insulin secretion (first-phase) which declined and was followed by a slow increase (second-phase) in insulin secretion. PAX6 knockdown markedly reduced GSIS in both first- and second-phases and overexpression of Munc18-1 or Munc18-2 tended to improve them (Fig. 2B). To examine whether reduced insulin secretion could be the result of a distal signaling defect, we measured potassium-stimulated insulin secretion (KSIS) in PAX6 knockdown cells. Similar to GSIS, KSIS was significantly impaired by PAX6 knockdown. Importantly, overexpression of Munc18-1 or Munc18-2 largely restored the KSIS defect (Fig. 2B). To further elucidate the interaction between PAX6 and Munc18-1/2 in regard to insulin secretion, we first generated stable Munc18-1 or Munc18-2 knockdown in EndoC-βH1 cells, then overexpressed PAX6 in these cells. As shown in Fig. S2C and S2D, reduced Munc18-1 and Munc18-2 protein levels by shRNA knockdown were enhanced by PAX6 overexpression. For insulin secretion, Munc18-1 or Munc18-2 knockdown resulted in decreased GSIS compared to the control group. PAX6 overexpression alone had no effect on GSIS, but could fully rescue the reduced insulin secretion associated with Munc18-1 or Munc18-2 knockdown (Fig. 2C). Dynamic measurement of insulin secretion further demonstrated that Munc18-1 and Munc18-2 knockdown reduced GSIS in both first- and second-phases while PAX6 overexpression could relieve the defects. Knockdown of Munc18-1 or Munc18-2 also suppressed KSIS where PAX6 overexpression tended to restore it (Fig. 2D). In addition, PAX6

knockdown also diminished insulin secretion induced by Exendin-4, a GLP-1 analog (Fig. S3B). This result further validated the essential role of PAX6 in insulin exocytosis, the final and common step of stimulated insulin secretion.

PAX6 regulates Munc18-1/2 expression via modulation of CREB signaling. The above results demonstrated that PAX6 modulated the expression of exocytotic proteins Munc18-1 and Munc18-2, which in turn affected insulin secretion. But how PAX6 regulates Munc18-1/2 expression is unclear. To examine whether both Munc18-1 and Munc18-2 are the direct targets of PAX6, we checked if the promoter regions of Munc18-1/2 contain PAX6 consensus binding site (TTCACGCATGAGTG) but did not identify any putative binding sites. Luciferase reporter assay using luciferase vectors carrying human *MUNC18-1* and *MUNC18-2* promoters with GFP or PAX6-overexpressing vector co-transfection also showed that PAX6 itself was unable to activate *MUNC18-1* and *MUNC18-2* promoters (Fig. S4A), suggesting that the regulation might depend on other factors. Several putative CREs had been identified in both mouse and human *MUNC18-1* and *MUNC18-2* promoters (Table S2). Luciferase reporter assay showed that CREB overexpression, raising phosphorylated and total CREB levels (Fig. S1D), drastically enhanced luciferase activity (Fig. 3A), indicating the transactivation of both *MUNC18-1* and *MUNC18-2* promoters by CREB. Of note, deletion of the putative CREs in both human *MUNC18-1* and *MUNC18-2* promoters reduced the transactivation by CREB overexpression, confirming the functionality of those CREs. Moreover, glucose and forskolin (FSK), the CREB activators, increased the promoter activity with effects weakened by ablation of CREs (Fig. S4C). Accordingly, chromatin immunoprecipitation assay showed that there was a significant enrichment of phospho-CREB to the CREs in both human *MUNC18-1* and *MUNC18-2* promoters (Fig. 3B), which revealed the physical bindings of phospho-CREB to both promoters.

CREB activation mediated by FSK or isobutylmethylxanthine (IBMX) greatly enhanced the binding of phospho-CREB to *MUNC18-1* and *MUNC18-2* promoters (Fig. S4B). Functionally, FSK and IBMX induced Munc18-1 and Munc18-2 expression at both mRNA and protein levels whereas CREB knockdown down-regulated their expression levels (Fig. S5). These data unravelled CREB as a direct transcriptional regulator of Munc18-1/2. To determine whether PAX6 modulates Munc18-1/2 expression via CREB signaling, regulation of CREB signaling by PAX6 was examined. As shown in Fig. 3C and S6A, PAX6 knockdown reduced total CREB protein level and the mRNA expression of some of the key CREB family members including *CREB* and *CREM* while PAX6 overexpression enhanced their mRNA levels. Blunted glucose-induced CREB phosphorylation (Ser133) and transcription of CREB target genes, *cFOS* and *NR4A1* (*32*) were observed in cells with PAX6 knockdown (Fig. 3C and S6B). Concomitantly, glucose-stimulated ATP and cAMP production as well as Ca^{2+} influx, which are the substrates for CREB activation, were suppressed by PAX6 knockdown (Fig. 3D, 3E and S6C), likely resulting from reduced expression of Glut1 (Fig. S8A), the predominant glucose transporter in human beta-cells (*33*). In particular, overexpression of CREB or CREB-regulated transcription coactivator 2 (CRTC2) prevented the down-regulation of both Munc18-1 and Munc18-2 caused by PAX6 knockdown (Fig. 3F, S7A and S7C) whereas CREB inhibition (666-15) prevented their up-regulation induced by PAX6 overexpression (Fig. 3G and S7B). These results indicated that the regulation of Munc18-1/2 expression by PAX6 is mostly CREB-dependent. For insulin secretion, CREB or CRTC2 overexpression preserved GSIS impaired by PAX6 knockdown (Fig. 3H). Collectively, these observations provided evidence that PAX6 regulated CREB signaling which in turn modulated Munc18-1/2 expression and insulin secretion at the functional level.

Repressed PAX6/CREB/Munc18 axis in pancreatic beta-cells under diabetic condition leads to blunted insulin secretion. As reduced GSIS is a hallmark of beta-cell dysfunction in T2D, we examined the potential participation of PAX6/CREB/Munc18 axis in T2D-associated defective GSIS by treating EndoC-βH1 cells or primary mouse islets with high glucose and palmitic acid (HGPA) which mimicked diabetic condition. Long-term (>48 h) HGPA treatment evidently attenuated protein levels of PAX6, Munc18-1 and Munc18-2 in both EndoC-βH1 cells and mouse islets (Fig. 4A); while these were alleviated by PAX6 restoration in cells (Fig. 4B and S7D). The involvement of CREB signaling was also investigated. Results showed that HGPA treatment prominently decreased Glut1 expression, inhibited glucose-induced ATP and cAMP production, Ca^{2+} influx as well as CREB Ser133 phosphorylation in EndoC-βH1 cells, all of which could be restored by PAX6 overexpression (Fig. S8B, 4C, 4D, S6D and 4E). As a downstream effector of PAX6, direct CREB or CRTC2 overexpression was able to counteract Munc18-1 and Munc18-2 down-regulation led by HGPA treatment (Fig. 4F and S7D), confirming the regulatory role of CREB in Munc18-1 and Munc18-2 expression under diabetic condition. For insulin secretion, 72 h-incubation of EndoC-βH1 cells in HGPA considerably suppressed GSIS while individual overexpression of PAX6, Munc18-1, Munc18-2, CREB or CRTC2 ameliorated the defect to varying extents (Fig. 4G). These data indicated that repressed PAX6/CREB/Munc18 axis in beta-cells contributed to compromised beta-cell function in diabetic condition.

Beta-cell specific PAX6 overexpression preserves CREB/Munc18-1/2 signaling pathway and GSIS in *db/db* mouse islets. The above results evidently illustrated the modulatory role of PAX6/CREB/Munc18 axis in beta-cell insulin secretion. We then substantiated their role in a real physiological situation using *db/db* mice, a rodent model of T2D. In agreement with the

observation in EndoC-βH1 cells under HGPA condition, isolated *db/db* mouse islets exhibited marked diminution in PAX6, Munc18-1 and Munc18-2 protein expression compared to *db/+* control mice (Fig. 5A). To elucidate the *in vivo* effects of PAX6 restoration in beta-cell function, 8-week-old *db/db* mice were injected with adeno-associated virus (AAV) overexpressing GFP control or PAX6 driven by the rat insulin promoter. Immunofluorescence staining showed that most of the exogenous PAX6 was expressed in beta-cells but not in alpha-cells with minimal effect on other internal organs (Fig. 5B, S9A and S9B). Western blotting further showed the presence of exogenous PAX6 in pancreatic islets 6 weeks after gene delivery (Fig. S9C and S9D). Of note, AAV-PAX6 counteracted the down-regulation of both Munc18-1 and Munc18-2 as well as Glut2 in *db/db* mouse islets (Fig. 5C and S8C). Glucose-induced ATP and cAMP production was abolished in *db/db* mouse islets compared to *db/+* control which was elevated by AAV-PAX6 (Fig. 5D and 5E). Concurrently, *db/db* mouse islets displayed attenuated CREB Ser133 phosphorylation upon high glucose stimulation which was again augmented by PAX6 overexpression (Fig. 5F). For insulin-secreting capacity, isolated *db/db* mouse islets had diminished GSIS which was substantially potentiated by AAV-PAX6 (Fig. 5G). Dynamic measurement of insulin release showed a significant decline in both first- and second-phases of GSIS in *db/db* mouse islets compared to *db/+* mouse islets while AAV-PAX6 prominently enhanced the first-phase of insulin secretion. KSIS was also weakened in *db/db* mouse islets, and this was largely recovered by AAV-PAX6 (Fig. 5H).

Beta-cell specific PAX6 overexpression improves glucose homeostasis in *db/db* mice. *Db/db* mouse islets displayed repressed PAX6/CREB/Munc18 axis correlated with impaired GSIS, which is fundamental to deteriorated glucose homeostasis in T2D, we hence examined the potential anti-diabetic effect of AAV-PAX6 in *db/db* mice *in vivo*. Strikingly, intraperitoneal

glucose tolerance test (IPGTT) showed that AAV-PAX6 improved glucose tolerance in *db/db* mice 2 weeks after injection and the effect was sustained for at least 6 weeks (Fig. 6A). Measurement of insulin secretion during IPGTT revealed that the early phase of insulin secretion was lost in *db/db* mice but was regained by AAV-PAX6 treatment (Fig. 6B). Hyperglycemia was also progressively alleviated without affecting weight gain (Fig. 6C and 6D). Given that peripheral insulin resistance is another factor contributing to glucose intolerance in T2D, insulin tolerance test (ITT) was performed to evaluate the effect of AAV-PAX6 on insulin sensitivity. As shown in Fig. 6E, insulin sensitivity in *db/db* mice was not influenced by beta-cell specific PAX6 overexpression, indicating that the moderation of glucose intolerance was mostly due to the potentiation of insulin secretion at those time points. Collectively, these results provided compelling evidence that restoration of the PAX6/CREB/Munc18 axis in islets promoted GSIS which in turn ameliorated glucose metabolism in diabetic mice.

Beta-cell specific PAX6 overexpression restores CREB/Munc18-1/2 signaling pathway and GSIS in T2D human islets. To determine whether reduction of islet PAX6 and Munc18-1/2 expression might occur in human T2D, we first determined the protein expression levels of PAX6 and Munc18-1/2 in islets from normal and T2D donors. In accordance with the results observed in *db/db* mice, the expression levels of PAX6, Munc18-1 and Munc18-2 were markedly decreased in T2D islets (Fig. 7A). AAV-PAX6 led to the expression of exogenous PAX6 mostly in beta-cells (Fig. S10A and S10B), noticeably restored the protein levels of Munc18-1 and Munc18-2 as well as Glut1 in T2D islets (Fig. 7B and S8D). Glucose-induced ATP and cAMP generation was dampened in T2D islets which was elevated by AAV-PAX6 (Fig. 7C and 7D). For CREB signaling, by contrast with the robust induction of Ser133 phosphorylation in normal islets, glucose had only modest effect on T2D islets which was

augmented by AAV-PAX6 (Fig. 7E). Functionally, GSIS was attenuated in T2D islets but could be mitigated by AAV-PAX6 (Fig. 7F). Dynamic measurement of insulin release showed an absence of the first-phase and a weakened second-phase of insulin release upon glucose challenge in T2D islets compared to normal islets; whereas a clear biphasic pattern of insulin release was regained by AAV-PAX6. The reduced KSIS in T2D islets was also enhanced by AAV-PAX6 (Fig. 7G). Overall, these results corroborated the existence of dampened PAX6/CREB/Munc18 axis in human T2D islets; while replenishment of PAX6 reversed those defects and potentiated GSIS.

Discussion

Impaired insulin secretion is a major feature of beta-cell failure determining the progression of insulin resistance to hyperglycemia and overt T2D, which has become a global public health threat. Therefore, gaining a better understanding of the molecular mechanism underlying beta-cell dysfunction is of paramount importance because it provides new insights into potential effective intervention strategies for T2D. Insulin secretion is a dynamic process and its regulation is highly complex, resulting from a combinatorial network of transcription factors. PAX6 is one of the major factors determining adult beta-cell function. PAX6 ablation in adult murine islet cells attenuates insulin production and secretion resulting in hyperglycemia and glucose intolerance (*5, 7, 8*). Mechanistic studies performed in rodent beta-cells demonstrated that PAX6 modulates the proximal signaling of GSIS including glucose sensing, ATP production and Ca^{2+} dynamics (*6, 8*). Most of the prior studies looked into the physiological roles of PAX6 in rodent beta-cells, however, whether PAX6 exerts the same functions in human beta-cells has not been demonstrated, there is also no direct evidence showing the involvement of PAX6 in human T2D. In this study, we made several novel observations concerning the role of PAX6 in beta-cell

function and T2D progression. Firstly, we provided *in vitro* and *ex vivo* evidence showing for the first time that PAX6 regulates both proximal and distal signaling of GSIS in human beta-cells by controlling glucose transport, ATP and cAMP production, Ca^{2+} influx, CREB activation and expression of exocytotic proteins Munc18-1 and Munc18-2. Secondly, we found that the PAX6/CREB/Munc18-1/2 axis is dampened in human pancreatic islets under T2D condition, unraveling the pathophysiological role of this axis in human diabetes. Thirdly, we showed that AAV-mediated replenishment of PAX6 prominently improved beta-cell function and alleviated glycemic disturbance in *db/db* mice *in vivo*.

Exocytosis is the final but the most critical step of insulin secretion. Various nutrients or stimuli trigger insulin secretion through different pathways but all converge on exocytosis to accomplish secretion. Cognate SM proteins are indispensable to execute insulin secretion in mouse and human islets (*27-29*). We have provided new evidence illustrating the regulatory role of PAX6 in the distal signaling of GSIS by modulating the expression of exocytotic proteins Munc18-1/2 in human beta-cells. Importantly, the present findings are in line with data from earlier studies (*8*). Thus, interrogation of the RNA-Seq data from the study reveals that *Stxbp1* (Munc18-1) mRNA was reduced highly significantly (~1.6 fold) in adult beta-cell-selective *Pax6* KO mice (*8*), though *Stxbp2* (Munc18-2) expression was not changed at the mRNA level. Our *in vitro* study using human beta-cell line demonstrated that Munc18-1/2 knockdown suppressed both GSIS and KSIS while PAX6 overexpression largely restored the defects. Conversely, PAX6 knockdown diminished Munc18-1/2 expression and suppressed both GSIS and KSIS. Overexpression of Munc18-1/2 could only partially rescue the reduced GSIS. This partial rescue is likely because PAX6 modulates both proximal and distal mechanisms of GSIS and overexpression of Munc18-

1/2 could only restore the distal mechanism, but not the proximal signaling caused by PAX6 knockdown.

We further demonstrated that CREB is the downstream mediator of PAX6 in controlling Munc18-1/2 expression. CREB is a transcription factor critical to maintain functional beta-cell mass by enhancing cell survival and preventing apoptosis. CREB specifically regulates the expression of crucial genes including Bcl-2, cyclins and insulin receptor substrate-2 (IRS-2) in beta-cells (*19, 20, 22, 34*). Although it is activated by a range of insulin-secreting stimuli such as glucose, GLP-1 and GIP (*23*), the role of CREB in insulin secretion remains elusive. In the present study, we uncovered Munc18-1 and Munc18-2 as the novel transcriptional targets of CREB. Putative CREs were identified in the promoter regions of both Munc18-1 and Munc18-2 genes in mouse and human. Most putative CREs identified locate within 200 nucleotides upstream of the transcription start sites which are defined as the proximal promoter regions, where the CREs are most likely to be functional. Frequent occurrence of CREs also indicates that they are highly conserved across species (*35*). The full CREs existing in human (TGACGCGC) and mouse (TGACGCGT) Munc18-2 promoters had been recognized in previous studies (*36, 37*); whilst the full CRE in human *MUNC18-1* promoter (TGACGCCA) has been shown to be a functional CRE (*38*). Chromatin immunoprecipitation study and luciferase reporter assay substantiated the physical binding and transactivation of human *MUNC18-1* and *MUNC18-2* promoters by CREB. Of note, our results showed that PAX6 knockdown in EndoC-βH1 cells reduced Glut1 expression, glucose-induced ATP/ cAMP generation and Ca^{2+} influx, which would in turn lead to repressed CREB activation. Indeed, PAX6 knockdown *per se* reduced the expression levels of CREB and other CREB family members which would further attenuate CREB activity. However, whether PAX6 regulates CREB expression by a direct transcriptional

modulation or through other signaling pathways requires further investigation. Functionally, PAX6 knockdown and overexpression resulting in Munc18-1/2 down- and up-regulation were counteracted by CREB overexpression/ activation and inhibition respectively. Impaired GSIS led by PAX6 knockdown and HGPA treatment was also relieved by CREB/ CRTC2 overexpression. Overall, apart from the reported regulatory role of PAX6 in the proximal signaling of GSIS, our results provide compelling evidence elucidating a previously unknown signaling network between PAX6 and CREB in the modulation of Munc18-1/2 expression, which underlies the role of PAX6 in the coordination of the proximal and distal signaling of GSIS.

Progressive deterioration of beta-cell function, particularly impairment of GSIS, is a central event driving T2D progression. To gain insights into the pathophysiological role of the PAX6/CREB/Munc18-1/2 axis in T2D-associated beta-cell dysfunction, EndoC-βH1 cells were exposed to HGPA to mimic T2D condition. HGPA down-regulated the entire pathway and suppressed GSIS which were rescued by restoration of PAX6 expression, indicating that dysregulation of the PAX6/CREB/Munc18-1/2 would be one of the pathways driving impaired GSIS under diabetic condition. The therapeutic potential of PAX6 in T2D was further delineated using *db/db* mice which exhibited prominently defective insulin secretion and frank diabetes. In line with the aforementioned *in vitro* results, the PAX6/CREB/Munc18-1/2 axis was repressed in *db/db* mouse islets. As there is no known specific agonist for PAX6, we adopted the AAV approach to restore PAX6 expression. Non-integrative AAV vectors, derived from non-pathogenic viruses, persist for years as episomes in nuclei of non-dividing cells (*39*). Multiple clinical studies have provided promising evidence of AAV-mediated long-term expression of therapeutic proteins without causing significant adverse effects (*40-42*). Here, we took advantage of AAV vectors and their ability to mediate long-term production of target proteins to develop a

gene therapy strategy for T2D based on PAX6 transfer to beta-cells. AAV-PAX6 potentiated the CREB/Munc18-1/2 axis, markedly enhanced the first-phase of GSIS *in vivo* and *ex vivo* while ameliorating glucose homeostasis in *db/db* mice. Improvement in glucose homeostasis could be observed 2 weeks after AAV injection and was sustained for least 6 weeks. To further explore the relevance of these findings to humans, we compared the axis in human islets between normal and T2D donors. Strikingly, a similar phenomenon had been observed in human islets. The PAX6/CREB/Munc18-1/2 axis was significantly dampened in T2D islets with impaired insulin secretion and PAX6 replenishment in beta-cells rescued the pathway and amplified both GSIS and KSIS. Our results unveiled the molecular link between PAX6 and CREB in the regulation of Munc18-1/2 expression and insulin secretion in human islets, in which attenuated PAX6 and CREB activity may explain the decrease in Munc18-1/2 expression under diabetic conditions (*28, 30, 31*). These observations further support the notion that PAX6 crucially determines beta-cell function in both mouse and human, while disruption of PAX6 expression or activity drives islet dysfunction and inflicts high risk to overt T2D progression.

Early and late phases of insulin secretion probably serve distinct physiological roles. Early phase response appears to efficiently suppress endogenous glucose production after meal while the late phase response predominately serves to enhance insulin-mediated glucose disposal in skeletal muscle and adipose tissue (*43, 44*). The progression from impaired glucose tolerance to frank diabetes is characterized by a dramatic decline in early insulin secretion as loss of early insulin secretion initially leads to postprandial hyperglycemia (*45, 46*). In this regard, by replenishing the upstream diminished modulator, AAV-PAX6 remarkably potentiated the first-phase of GSIS in diabetic mouse and human islets by targeting glucose transport, ATP/ cAMP generation and insulin exocytosis, thus restraining the deterioration of hyperglycemia in *db/db* mice. Although

AAV-PAX6 might not fully reverse T2D in mice, this strategy mitigated beta-cell dysfunction, one of the major contributors to T2D and demonstrated its potential in sustained alleviation of glycemic disturbance in T2D. Additionally, loss of beta-cell identity (dedifferentiation) is an emerging mechanism contributing to beta-cell dysfunction in T2D (*47*), while PAX6 has been demonstrated to maintain beta-cell identity and to repress alternative islet cell genes (*7*). Apart from the regulation of insulin secretion, further investigation on human beta-cell dedifferentiation is warranted to gain better understanding on the effects of PAX6 replenishment. It would also be important to investigate how PAX6 expression or activity is regulated. Identification of candidates that critically confer blunted PAX6 action in beta-cells under diabetic condition would aid the development of novel, effective therapy against T2D.

In summary, the present study advances the understanding of PAX6 as an indispensable transcription factor controlling GSIS in human pancreatic beta-cells through coordination of the proximal and distal signaling. Our results also shed light onto the pathophysiological role of PAX6 in T2D and provide new insights and scientific basis to support the future clinical translation of PAX6 gene transfer to overcome beta-cell failure in T2D.

Materials and Methods

Study Design. This study aimed to examine the molecular pathway of PAX6 in the regulation of insulin secretion, the pathophysiological role of PAX6 in beta-cell dysfunction and the potential therapeutic value of PAX6 in T2D. We performed loss- and gain-of-function studies using human EndoC-βH1 cell line to investigate the regulatory role of PAX6 in GSIS and the molecular mechanism. Type 2 diabetic *db/db* mice and primary human islets from normal and T2D donors were used to study the link between PAX6 and T2D-associated beta-cell failure.

Beta-cell specific overexpression of PAX6 was achieved by AAV administration. Glucose homeostasis of *db/db* mice and their lean control was monitored by IPGTT and ITT with insulin-secreting capacity evaluated. Islets were harvested at the endpoint for mechanistic studies. Mice were randomly divided into different groups and no animals were excluded because of illness. All experimental procedures involving animals were approved by the Institutional Animal Care and Use Committee in at A*STAR (Ref. No. 191479). All procedures involving human tissues were approved by A*STAR Institutional Review Board (Ref. No. 2019-021). All experiments were performed in at least triplicate biological repeats.

Cell culture. The human EndoC-βH1 cell line (Univercell-Biosolutions, Toulouse, France) was cultured as previously described (*48*). Cells were maintained under normal condition (5.6 mmol/l glucose) or treated with HGPA (25 mmol/l D-glucose and 0.3 mmol/l palmitic acid).

Lentivirus-mediated gene overexpression and knockdown. For gene overexpression, coding sequences expressing human *PAX6*, *MUNC18-1*, *MUNC18-2*, *CREB1* (OriGene, Rockville, MD, USA) and *CRTC2* (VectorBuilder, Santa Clara, CA, USA) were subcloned into the lentiviral pLV vector (Addgene, Cambridge, MA, USA) to generate overexpression constructs. For gene knockdown, shRNA sequences targeting human *PAX6*, *MUNC18-1*, *MUNC18-2* and *CREB1* (Table S1) were subcloned into the lentiviral pLKO.1 vector (Addgene) to generate knockdown constructs. Three shRNA sequences were used to knock down each of the gene with the sequence showing the highest knockdown efficiency chosen for downstream experiments (Fig. S1A-S1C). A non-targeting shRNA sequence was used as control. All DNA constructs were validated by sequencing. Viral particles were generated by transient transfection of HEK-293FT cells (American Type Culture Collection, Manassas, VA, USA) with the lentiviral plasmids and helper plasmids (pRSV-Rev, pCMV-VSVG and pMDLg/pRRE; Addgene) using lipofectamine

2000 reagent (Thermo Fisher Scientific, Rockford, IL, USA). The cell supernatant was collected, concentrated and titrated at 48 h post-transfection. EndoC-βH1 cells were infected with overexpressing or shRNA viral particles and were subjected to antibiotic selection to generate stable cell lines. For double infections, stable knockdown cell lines were first generated followed by overexpression. Viral particles carrying different selection markers (puromycin for knockdown and blasticidin for overexpression) were used.

Animal models. Male genetically diabetic C57BL/KsJ-db (*db*/*db*) and their age-matched, lean heterozygote littermates (*db*/+) were obtained from the Jackson Laboratory (Bar Harbor, ME, USA). Animals were fed *ad libitum* and maintained in a specific pathogen free facility with constant ambient temperature and a 12-h light/dark cycle.

Administration of AAV. The AAV8 carrying PAX6-flag-GFP (AAV-PAX6) or GFP only (AAV-Ctrl) driven by the rat insulin promoter was purchased from VectorBuilder. AAV-PAX6 or AAV-Ctrl was injected intraperitoneally into *db*/+ and *db/db* mice (8-week-old) at the dose of 1×10^{11} viral genomes (vg) per mouse as previously described (*49, 50*). Mice were observed for 6 weeks after AAV injection with pancreatic islets and organs isolated for analyses at the end point.

***In vivo* glucose homeostasis.** Glucose tolerance was assessed by IPGTT. After 16 h fasting, mice were given 1 g/kg body weight of glucose (Sigma-Aldrich, St. Louis, MO, USA) by intraperitoneal injection. Blood glucose and serum insulin levels were measured at the indicated time points. The first- and second-phases of insulin secretion were defined as 0-15 and 15-60 min respectively. For ITT, mice were injected with insulin (1 U/kg body weight; Sigma-Aldrich) after 4 h fasting and blood glucose levels were subsequently measured.

Pancreatic islet isolation, primary culture and treatments. Intact pancreatic islets were isolated from mice as previously described (*51*). Briefly, mouse pancreas was given an intra-ductal injection of collagenase P (Roche, Mannheim, Germany) in Hanks' balanced salt solution (Gibco, Grand Island, NY, USA). The pancreas was removed and digested in 37℃. After washing and gradient centrifugation, the islets were handpicked under a stereomicroscope. Isolated islets were further dispersed into single cells by trypsin digestion for ATP/ADP and cAMP measurement. Intact islets or dispersed cells were then cultured overnight for recovery in RPMI-1640 medium (Thermo Fisher Scientific) supplemented with 10% (vol/vol) fetal bovine serum (FBS; Gibco) and 1% (vol/vol) penicillin and streptomycin (Thermo Fisher Scientific).

Human islets, culture and transduction. Primary human islets from 4 normal and 4 T2D donors were obtained from Prodo Laboratories, Inc. (Aliso Viejo, CA, USA). Human islets were cultured in PIM(S) complete media (Prodo Labs) and transduced with AAV-Ctrl or AAV-PAX6 at a dose of 20 000 vg per islet cell.

Quantitative real-time PCR. Total RNA from cell samples was extracted using TRIzol reagent (Thermo Fisher Scientific) and subjected to reverse transcription using High-Capacity cDNA Reverse Transcription Kits (Applied Biosystems, Foster City, CA, USA). Gene expression was quantified by real-time PCR using SYBR^{TM} Green PCR Master Mix (Applied Biosystems). The reactions were performed using an i-Cycler Thermal Cycler (Applied Biosystems). Relative gene expression was analyzed using the $2^{(-\Delta\Delta Ct)}$ method and normalized relative to beta-actin. The sequences of primers used are listed in Table S1.

Western blotting. Proteins from isolated islets or organs were extracted using the RIPA Lysis and Extraction Buffer (Thermo Fisher Scientific). Proteins were separated by SDS-PAGE,

transferred to nitrocellulose membrane by iBlot™ 2 Gel Transfer Device (Thermo Fisher Scientific). After blocking, the membrane was incubated with antibodies against the following proteins: GAPDH (sc-32233; Santa Cruz Biotechnology Inc., Santa Cruz, CA, USA), phospho-CREB (9198; Cell Signaling, Danvers, MA, USA), CREB (9197; Cell Signaling), CRTC2 (ab109081; Abcam, Cambridge, MA, USA), PAX6 (ab197768; Abcam), Munc18-1 (ab109023; Abcam), Munc18-2 (ab97598; Abcam and GTX33529; Genetex Inc., Irvine, CA, USA), Glut1 (ab40084; Abcam), Glut2 (ab54460; Abcam) or Flag (F1804; Sigma-Aldrich). After washing, the membrane was incubated with appropriate IR-Dye labeled secondary antibodies (LI-COR Biosciences, Lincoln, NE, USA). Labeled protein bands were visualized and quantitated by Odyssey® CLx Imager (LI-COR Biosciences).

Insulin secretion assay. For static insulin release, cells or size-matched isolated islets were pre-incubated in Krebs-Ringer bicarbonate buffer (KRBB; supplemented with 10 mmol/l HEPES and 2 mg/ml BSA) with 2.5 mmol/l glucose for 1 h followed by incubation in KRBB containing 2.5 mmol/l or 16.7 mmol/l glucose for an additional 1 h, as described previously (*51*). Buffer was collected to measure insulin release by ELISA kits (Antibody and Immunoassay Services, University of Hong Kong, Hong Kong, China). For dynamic insulin release, cells or isolated islets were perifused with KRBB containing 2.5 mmol/l or 16.7 mmol/l glucose or 20 mmol/l KCl at a constant flow rate for the indicated periods of time. The first- and second-phases of insulin secretion were defined as 0-12 and 12-30 min respectively. Eluted fractions were collected to measure insulin release.

Luciferase reporter assay. DNA fragments corresponding to the promoter regions of human *MUNC18-1* and *MUNC18-2* genes were amplified by PCR from EndoC-βH1 cell genomic DNA using primers listed in Table S1. The PCR products were subcloned into the pGL3-basic

luciferase reporter vector (Promega, Madison, WI, USA). All constructs were validated by sequencing. EndoC-βH1 cells were co-transfected with the reporter/ control vector, a pRL-TK renilla luciferase vector (Promega) and a CREB-overexpressing/ control vector using Lipofectamine 2000 for 48 h. Cells were subjected to luciferase activity measurement by a dual-luciferase reporter assay kit (Promega) on a luminometer (Promega). The firefly luciferase activity was normalized against renilla luciferase activity.

Chromatin immunoprecipitation. EndoC-βH1 cells were fixed in 1% formaldehyde. Crosslinking reaction was stopped by glycine at 125 mmol/l final concentration. Cells were lysed and nuclear fraction was extracted for sonication to shear DNA fragments in the range of 200-600bp. Cell lysate was then subjected to immunoprecipitation with magnetic beads (Thermo Fisher Scientific) coated with anti-phospho-CREB antibody or normal rabbit IgG (Merck Millipore, Darmstadt, Germany) overnight at 4℃. The complex was washed and eluted with elution buffer (1% SDS and 0.1 M $NaHCO_3$). The crosslinks were reversed by incubating the complex at 65℃ overnight followed by DNA purification using QIAquick PCR Purification Kit (Qiagen, Hilden, Germany). The DNA fragments were analyzed by quantitative real-time PCR using primers targeting human *MUNC18-1* and *MUNC18-2* gene promoters. Primers targeting *GAPDH* region containing no CRE were used as negative control. All primers used are listed in Table S1.

Measurement of intracellular ATP/ADP ratio and cAMP level. EndoC-βH1 cells or dispersed islet cells were pre-incubated in KRBB with 2.5 mmol/l glucose for 1 h followed by stimulation with 2.5 mmol/l or 20 mmol/l glucose for 15 min. The relative ATP/ADP content and cAMP level were measured using the ADP/ATP ratio assay kit (Abcam) and cAMP immunoassay kit (Sigma-Aldrich) according to manufacturers' instructions.

Immunofluorescence staining. Isolated islets and organs were embedded and frozen. Cryostat sections were collected and fixed. Slides were incubated with mouse anti-flag (F1804; Sigma-Aldrich), guinea pig anti-insulin (PA1-26938; Thermo Fisher Scientific), rabbit anti-glucagon (ab92517; Abcam) and chicken anti-GFP (GFP-1020; Aves Labs, Tigard, OR, USA) antibodies. After washing, slides were probed with Alexa Fluor dye-conjugated secondary antibodies (Thermo Fisher Scientific). Slides were mounted with antifade mountant with DAPI (Thermo Fisher Scientific) before image acquirement. Digital images were acquired by a Ti-E fluorescence microscope (Nikon, Tokyo, Japan).

Ca^{2+} imaging. EndoC-βH1 cells were transfected with the GCaMP7s vector (addgene) using Lipofectamine 2000 for 48 h. EndoC-βH1 cells were pre-incubated in KRBB with 2.5 mmol/l glucose for 1 h followed by stimulation with 20 mmol/l glucose. A Ti-E fluorescence microscope (Nikon) was used for live cell imaging. Image analysis was performed using the NIS-Elements (Nikon) software.

Statistical analysis. Data were expressed as means ± standard errors (SEMs). Comparisons between groups were analyzed by two-tailed Student's *t* test, one-way or two-way analysis of variance (ANOVA) followed by Tukey's *post hoc* test, where $p<0.05$ was considered statistically significant.

Supplementary Materials

Fig. S1. Western blotting showing shRNA knockdown efficiency and CREB overexpression in EndoC-βH1 cells.

Fig. S2. Western blotting showing protein expression of Munc18-1/2 in EndoC-βH1 cells with manipulation of PAX6 and Munc18-1/2.

Fig. S3. Effects of PAX6 knockdown on insulin content and Exendin-4-induced insulin secretion in EndoC-βH1 cells.

Fig. S4. Luciferase activity of human *MUNC18-1* and *MUNC18-2* promoters and chromatin immunoprecipitation assay showing binding of pCREB onto human *MUNC18-1* and *MUNC18-2* promoters.

Fig. S5. CREB phosphorylation, protein and mRNA levels of Munc18-1/2 in EndoC-βH1 cells after CREB activation or knockdown.

Fig. S6. PAX6's regulation of CREB family member gene expression, CREB target gene induction and Ca^{2+} influx.

Fig. S7. Effects of CREB signaling regulation on Munc18-1/2 expression in EndoC-βH1 cells.

Fig. S8. Western blotting showing Glut1 and Glut2 protein expression.

Fig. S9. The expression of exogenous PAX6 in mice receiving AAV-PAX6.

Fig. S10. The expression of exogenous PAX6 in human islets with AAV-PAX6 treatment.

Table S1. Oligonucleotide sequences used in shRNA vectors construction, quantitative real-time PCR, luciferase vectors construction and ChIP assay.

Table S2. Sequences and positions of putative CREs in promoters of Munc18-1 and Munc18-2 in both human and mouse.

Table S3. Human islet donor information.

References

1. G. I. Bell, K. S. Polonsky, Diabetes mellitus and genetically programmed defects in beta-cell function. *Nature* **414**, 788-791 (2001).
2. J. E. Gerich, The genetic basis of type 2 diabetes mellitus: impaired insulin secretion versus impaired insulin sensitivity. *Endocr Rev* **19**, 491-503 (1998).
3. M. Sander, A. Neubuser, J. Kalamaras, H. C. Ee, G. R. Martin, M. S. German, Genetic analysis reveals that PAX6 is required for normal transcription of pancreatic hormone genes and islet development. *Genes Dev* **11**, 1662-1673 (1997).
4. L. St-Onge, B. Sosa-Pineda, K. Chowdhury, A. Mansouri, P. Gruss, Pax6 is required for differentiation of glucagon-producing alpha-cells in mouse pancreas. *Nature* **387**, 406-409 (1997).
5. Z. Ahmad, M. Rafeeq, P. Collombat, A. Mansouri, Pax6 Inactivation in the Adult Pancreas Reveals Ghrelin as Endocrine Cell Maturation Marker. *PLoS One* **10**, e0144597 (2015).
6. Y. Gosmain, L. S. Katz, M. H. Masson, C. Cheyssac, C. Poisson, J. Philippe, Pax6 is crucial for beta-cell function, insulin biosynthesis, and glucose-induced insulin secretion. *Mol Endocrinol* **26**, 696-709 (2012).
7. A. Swisa, D. Avrahami, N. Eden, J. Zhang, E. Feleke, T. Dahan, Y. Cohen-Tayar, M. Stolovich-Rain, K. H. Kaestner, B. Glaser, R. Ashery-Padan, Y. Dor, PAX6 maintains beta cell identity by repressing genes of alternative islet cell types. *J Clin Invest* **127**, 230-243 (2017).
8. R. K. Mitchell, M. S. Nguyen-Tu, P. Chabosseau, R. M. Callingham, T. J. Pullen, R. Cheung, I. Leclerc, D. J. Hodson, G. A. Rutter, The transcription factor Pax6 is required for pancreatic beta cell identity, glucose-regulated ATP synthesis, and Ca(2+) dynamics in adult mice. *J Biol Chem* **292**, 8892-8906 (2017).
9. R. Ashery-Padan, X. Zhou, T. Marquardt, P. Herrera, L. Toube, A. Berry, P. Gruss, Conditional inactivation of Pax6 in the pancreas causes early onset of diabetes. *Dev Biol* **269**, 479-488 (2004).
10. T. Yasuda, Y. Kajimoto, Y. Fujitani, H. Watada, S. Yamamoto, T. Watarai, Y. Umayahara, M. Matsuhisa, S. Gorogawa, Y. Kuwayama, Y. Tano, Y. Yamasaki, M. Hori, PAX6 mutation as a genetic factor common to aniridia and glucose intolerance. *Diabetes* **51**, 224-230 (2002).
11. M. Nishi, M. Sasahara, T. Shono, S. Saika, Y. Yamamoto, K. Ohkawa, H. Furuta, T. Nakao, H. Sasaki, K. Nanjo, A case of novel de novo paired box gene 6 (PAX6) mutation with early-onset diabetes mellitus and aniridia. *Diabet Med* **22**, 641-644 (2005).
12. S. Motoda, S. Fujita, J. Kozawa, T. Kimura, K. Fukui, Y. Ikuno, A. Imagawa, H. Iwahashi, I. Shimomura, Case of a novel PAX6 mutation with aniridia and insulin-dependent diabetes mellitus. *J Diabetes Investig*, (2018).
13. N. Gustavsson, W. Han, Calcium-sensing beyond neurotransmitters: functions of synaptotagmins in neuroendocrine and endocrine secretion. *Biosci Rep* **29**, 245-259 (2009).
14. S. Seino, T. Shibasaki, PKA-dependent and PKA-independent pathways for cAMP-regulated exocytosis. *Physiol Rev* **85**, 1303-1342 (2005).
15. W. A. Carlezon, Jr., R. S. Duman, E. J. Nestler, The many faces of CREB. *Trends Neurosci* **28**, 436-445 (2005).
16. A. J. Shaywitz, M. E. Greenberg, CREB: a stimulus-induced transcription factor activated by a diverse array of extracellular signals. *Annu Rev Biochem* **68**, 821-861 (1999).
17. P. Sassone-Corsi, Transcription factors responsive to cAMP. *Annu Rev Cell Dev Biol* **11**, 355-377 (1995).
18. M. Comb, N. C. Birnberg, A. Seasholtz, E. Herbert, H. M. Goodman, A cyclic AMP- and phorbol ester-inducible DNA element. *Nature* **323**, 353-356 (1986).

19. U. S. Jhala, G. Canettieri, R. A. Screaton, R. N. Kulkarni, S. Krajewski, J. Reed, J. Walker, X. Lin, M. White, M. Montminy, cAMP promotes pancreatic beta-cell survival via CREB-mediated induction of IRS2. *Genes Dev* **17**, 1575-1580 (2003).
20. S. J. Kim, C. Nian, S. Widenmaier, C. H. McIntosh, Glucose-dependent insulinotropic polypeptide-mediated up-regulation of beta-cell antiapoptotic Bcl-2 gene expression is coordinated by cyclic AMP (cAMP) response element binding protein (CREB) and cAMP-responsive CREB coactivator 2. *Mol Cell Biol* **28**, 1644-1656 (2008).
21. A. Inada, Y. Hamamoto, Y. Tsuura, J. Miyazaki, S. Toyokuni, Y. Ihara, K. Nagai, Y. Yamada, S. Bonner-Weir, Y. Seino, Overexpression of inducible cyclic AMP early repressor inhibits transactivation of genes and cell proliferation in pancreatic beta cells. *Mol Cell Biol* **24**, 2831-2841 (2004).
22. S. A. Sarkar, J. Gunter, R. Bouchard, J. E. Reusch, A. Wiseman, R. G. Gill, J. C. Hutton, S. Pugazhenthi, Dominant negative mutant forms of the cAMP response element binding protein induce apoptosis and decrease the anti-apoptotic action of growth factors in human islets. *Diabetologia* **50**, 1649-1659 (2007).
23. S. Dalle, J. Quoyer, E. Varin, S. Costes, Roles and regulation of the transcription factor CREB in pancreatic beta -cells. *Curr Mol Pharmacol* **4**, 187-195 (2011).
24. Y. A. Chen, S. J. Scales, S. M. Patel, Y. C. Doung, R. H. Scheller, SNARE complex formation is triggered by Ca2+ and drives membrane fusion. *Cell* **97**, 165-174 (1999).
25. N. Takahashi, H. Hatakeyama, H. Okado, J. Noguchi, M. Ohno, H. Kasai, SNARE conformational changes that prepare vesicles for exocytosis. *Cell Metab* **12**, 19-29 (2010).
26. R. Jahn, R. H. Scheller, SNAREs--engines for membrane fusion. *Nat Rev Mol Cell Biol* **7**, 631-643 (2006).
27. E. Oh, M. A. Kalwat, M. J. Kim, M. Verhage, D. C. Thurmond, Munc18-1 regulates first-phase insulin release by promoting granule docking to multiple syntaxin isoforms. *J Biol Chem* **287**, 25821-25833 (2012).
28. T. Qin, T. Liang, D. Zhu, Y. Kang, L. Xie, S. Dolai, S. Sugita, N. Takahashi, C. G. Ostenson, K. Banks, H. Y. Gaisano, Munc18b Increases Insulin Granule Fusion, Restoring Deficient Insulin Secretion in Type-2 Diabetes Human and Goto-Kakizaki Rat Islets with Improvement in Glucose Homeostasis. *EBioMedicine* **16**, 262-274 (2017).
29. D. Zhu, L. Xie, N. Karimian, T. Liang, Y. Kang, Y. C. Huang, H. Y. Gaisano, Munc18c mediates exocytosis of pre-docked and newcomer insulin granules underlying biphasic glucose stimulated insulin secretion in human pancreatic beta-cells. *Mol Metab* **4**, 418-426 (2015).
30. W. Zhang, A. Khan, C. G. Ostenson, P. O. Berggren, S. Efendic, B. Meister, Down-regulated expression of exocytotic proteins in pancreatic islets of diabetic GK rats. *Biochem Biophys Res Commun* **291**, 1038-1044 (2002).
31. C. G. Ostenson, H. Gaisano, L. Sheu, A. Tibell, T. Bartfai, Impaired gene and protein expression of exocytotic soluble N-ethylmaleimide attachment protein receptor complex proteins in pancreatic islets of type 2 diabetic patients. *Diabetes* **55**, 435-440 (2006).
32. D. M. Fass, J. E. Butler, R. H. Goodman, Deacetylase activity is required for cAMP activation of a subset of CREB target genes. *J Biol Chem* **278**, 43014-43019 (2003).
33. A. De Vos, H. Heimberg, E. Quartier, P. Huypens, L. Bouwens, D. Pipeleers, F. Schuit, Human and rat beta cells differ in glucose transporter but not in glucokinase gene expression. *J Clin Invest* **96**, 2489-2495 (1995).
34. M. J. Kim, J. H. Kang, Y. G. Park, G. R. Ryu, S. H. Ko, I. K. Jeong, K. H. Koh, D. J. Rhie, S. H. Yoon, S. J. Hahn, M. S. Kim, Y. H. Jo, Exendin-4 induction of cyclin D1 expression in INS-1 beta-cells: involvement of cAMP-responsive element. *J Endocrinol* **188**, 623-633 (2006).

35. B. Mayr, M. Montminy, Transcriptional regulation by the phosphorylation-dependent factor CREB. *Nat Rev Mol Cell Biol* **2**, 599-609 (2001).
36. R. Nigam, J. Sepulveda, M. Tuvim, Y. Petrova, R. Adachi, B. F. Dickey, A. Agrawal, Expression and transcriptional regulation of Munc18 isoforms in mast cells. *Biochim Biophys Acta* **1728**, 77-83 (2005).
37. K. Kim, Y. M. Petrova, B. L. Scott, R. Nigam, A. Agrawal, C. M. Evans, Z. Azzegagh, A. Gomez, E. M. Rodarte, V. M. Olkkonen, R. Bagirzadeh, L. Piccotti, B. Ren, J. H. Yoon, J. A. McNew, R. Adachi, M. J. Tuvim, B. F. Dickey, Munc18b is an essential gene in mice whose expression is limiting for secretion by airway epithelial and mast cells. *Biochem J* **446**, 383-394 (2012).
38. N. S. Foulkes, J. Borjigin, S. H. Snyder, P. Sassone-Corsi, Transcriptional control of circadian hormone synthesis via the CREM feedback loop. *Proc Natl Acad Sci U S A* **93**, 14140-14145 (1996).
39. F. Mingozzi, K. A. High, Therapeutic in vivo gene transfer for genetic disease using AAV: progress and challenges. *Nat Rev Genet* **12**, 341-355 (2011).
40. F. Testa, A. M. Maguire, S. Rossi, E. A. Pierce, P. Melillo, K. Marshall, S. Banfi, E. M. Surace, J. Sun, C. Acerra, J. F. Wright, J. Wellman, K. A. High, A. Auricchio, J. Bennett, F. Simonelli, Three-year follow-up after unilateral subretinal delivery of adeno-associated virus in patients with Leber congenital Amaurosis type 2. *Ophthalmology* **120**, 1283-1291 (2013).
41. A. C. Nathwani, U. M. Reiss, E. G. Tuddenham, C. Rosales, P. Chowdary, J. McIntosh, M. Della Peruta, E. Lheriteau, N. Patel, D. Raj, A. Riddell, J. Pie, S. Rangarajan, D. Bevan, M. Recht, Y. M. Shen, K. G. Halka, E. Basner-Tschakarjan, F. Mingozzi, K. A. High, J. Allay, M. A. Kay, C. Y. Ng, J. Zhou, M. Cancio, C. L. Morton, J. T. Gray, D. Srivastava, A. W. Nienhuis, A. M. Davidoff, Long-term safety and efficacy of factor IX gene therapy in hemophilia B. *N Engl J Med* **371**, 1994-2004 (2014).
42. J. W. Bainbridge, M. S. Mehat, V. Sundaram, S. J. Robbie, S. E. Barker, C. Ripamonti, A. Georgiadis, F. M. Mowat, S. G. Beattie, P. J. Gardner, K. L. Feathers, V. A. Luong, S. Yzer, K. Balaggan, A. Viswanathan, T. J. de Ravel, I. Casteels, G. E. Holder, N. Tyler, F. W. Fitzke, R. G. Weleber, M. Nardini, A. T. Moore, D. A. Thompson, S. M. Petersen-Jones, M. Michaelides, L. I. van den Born, A. Stockman, A. J. Smith, G. Rubin, R. R. Ali, Long-term effect of gene therapy on Leber's congenital amaurosis. *N Engl J Med* **372**, 1887-1897 (2015).
43. L. Luzi, R. A. DeFronzo, Effect of loss of first-phase insulin secretion on hepatic glucose production and tissue glucose disposal in humans. *Am J Physiol* **257**, E241-246 (1989).
44. R. E. Pratley, C. Weyer, The role of impaired early insulin secretion in the pathogenesis of Type II diabetes mellitus. *Diabetologia* **44**, 929-945 (2001).
45. S. Seino, T. Shibasaki, K. Minami, Dynamics of insulin secretion and the clinical implications for obesity and diabetes. *J Clin Invest* **121**, 2118-2125 (2011).
46. R. E. Pratley, C. Weyer, Progression from IGT to type 2 diabetes mellitus: the central role of impaired early insulin secretion. *Curr Diab Rep* **2**, 242-248 (2002).
47. Y. Dor, B. Glaser, beta-cell dedifferentiation and type 2 diabetes. *N Engl J Med* **368**, 572-573 (2013).
48. P. Ravassard, Y. Hazhouz, S. Pechberty, E. Bricout-Neveu, M. Armanet, P. Czernichow, R. Scharfmann, A genetically engineered human pancreatic beta cell line exhibiting glucose-inducible insulin secretion. *J Clin Invest* **121**, 3589-3597 (2011).
49. C. Zhao, C. Qiao, R. H. Tang, J. Jiang, J. Li, C. B. Martin, K. Bulaklak, D. W. Wang, X. Xiao, Overcoming Insulin Insufficiency by Forced Follistatin Expression in beta-cells of db/db Mice. *Mol Ther* **23**, 866-874 (2015).
50. K. Araki, A. Araki, D. Honda, T. Izumoto, A. Hashizume, Y. Hijikata, S. Yamada, Y. Iguchi, A. Hara, K. Ikumi, K. Kawai, S. Ishigaki, Y. Nakamichi, S. Tsunekawa, Y. Seino, A. Yamamoto, Y. Takayama, S.

Hidaka, M. Tominaga, M. Ohara-Imaizumi, A. Suzuki, H. Ishiguro, A. Enomoto, M. Yoshida, H. Arima, S. I. Muramatsu, G. Sobue, M. Katsuno, TDP-43 regulates early-phase insulin secretion via CaV1.2-mediated exocytosis in islets. *J Clin Invest* **130**, 3578-3593 (2019).

51. W. Y. So, Q. Cheng, A. Xu, K. S. Lam, P. S. Leung, Loss of fibroblast growth factor 21 action induces insulin resistance, pancreatic islet hyperplasia and dysfunction in mice. *Cell Death Dis* **6**, e1707 (2015).

Funding: W.H. is supported by intramural funding from the A*STAR Biomedical Research Council. W.Y.S. is supported by the Young Individual Research Grant (NMRC/OFYIRG/066/2018-00) from the National Medical Research Council, Singapore. G.A.R. was supported by a Wellcome Trust Investigator Award (212625/Z/18/Z), MRC Programme grants (MR/R022259/1, MR/J0003042/1, MR/L020149/1) and by Diabetes UK (BDA/11/0004210, BDA/15/0005275, BDA 16/0005485) project grants. This project has received funding from the European Union's Horizon 2020 research and innovation programme via the Innovative Medicines Initiative 2 Joint Undertaking under grant agreement No 115881 (RHAPSODY) to G.A.R. This Joint Undertaking receives support from the European Union's Horizon 2020 research and innovation programme and EFPIA. **Author contributions:** W.Y.S. designed and performed experiments, analyzed and interpreted data, and wrote the manuscript. W.N.L. performed experiments. A.K.K.T. edited and revised the manuscript. G.A.R. designed experiments, edited and revised the manuscript. W.H. designed the experiments, analyzed and interpreted data, edited and revised the manuscript. **Competing interests:** The authors declare no conflict of interest. **Data and materials availability:** All data associated with this study are present in the paper or the Supplementary Materials.

Figures

Figure 1

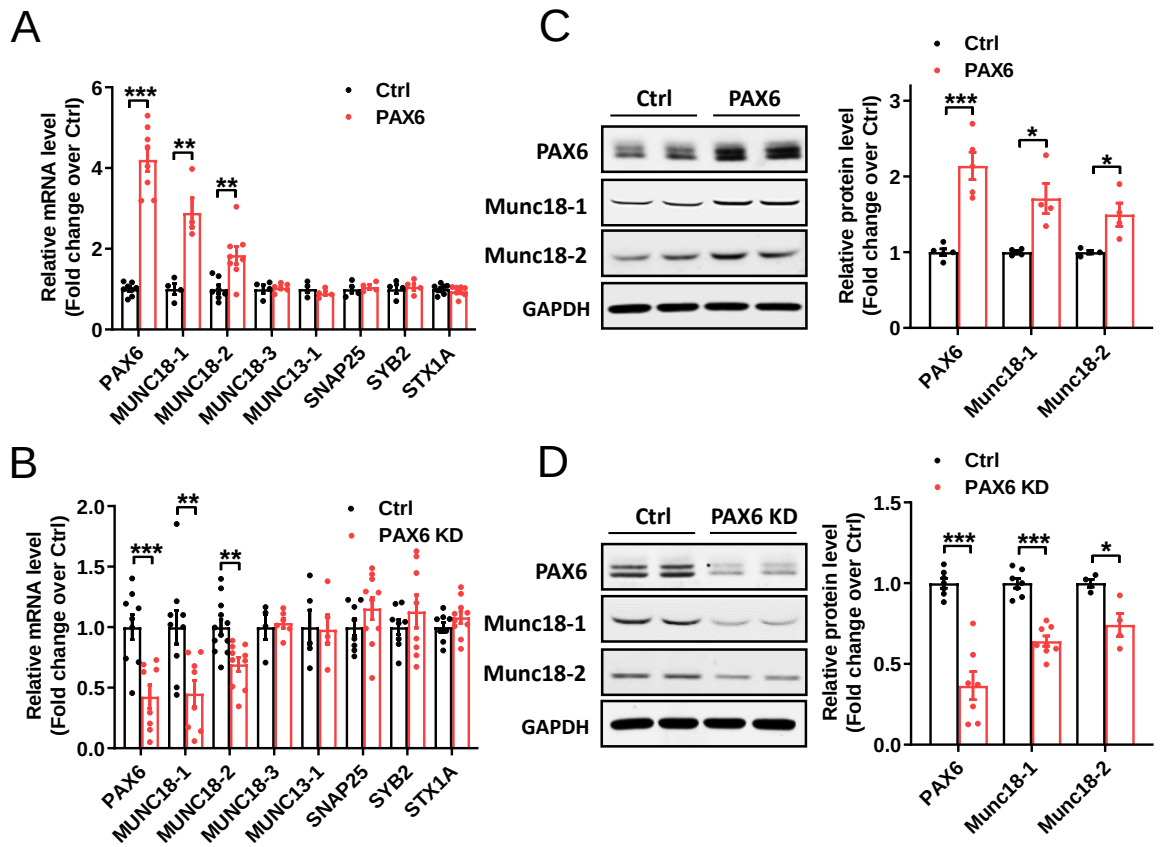

Fig. 1. PAX6 regulates Munc18-1/2 expression in human pancreatic beta-cells. mRNA expression levels of *PAX6* and exocytotic proteins in EndoC-βH1 cells with lentivirus-mediated PAX6 (A) overexpression and (B) knockdown (KD) (n=4-12). Protein expression levels of PAX6 and Munc18-1/2 in EndoC-βH1 cells with lentivirus-mediated PAX6 (C) overexpression and (D) knockdown. *P<0.05; **P<0.01; ***P<0.001 (n=4-8). Data are means ± SEMs.

Figure 2

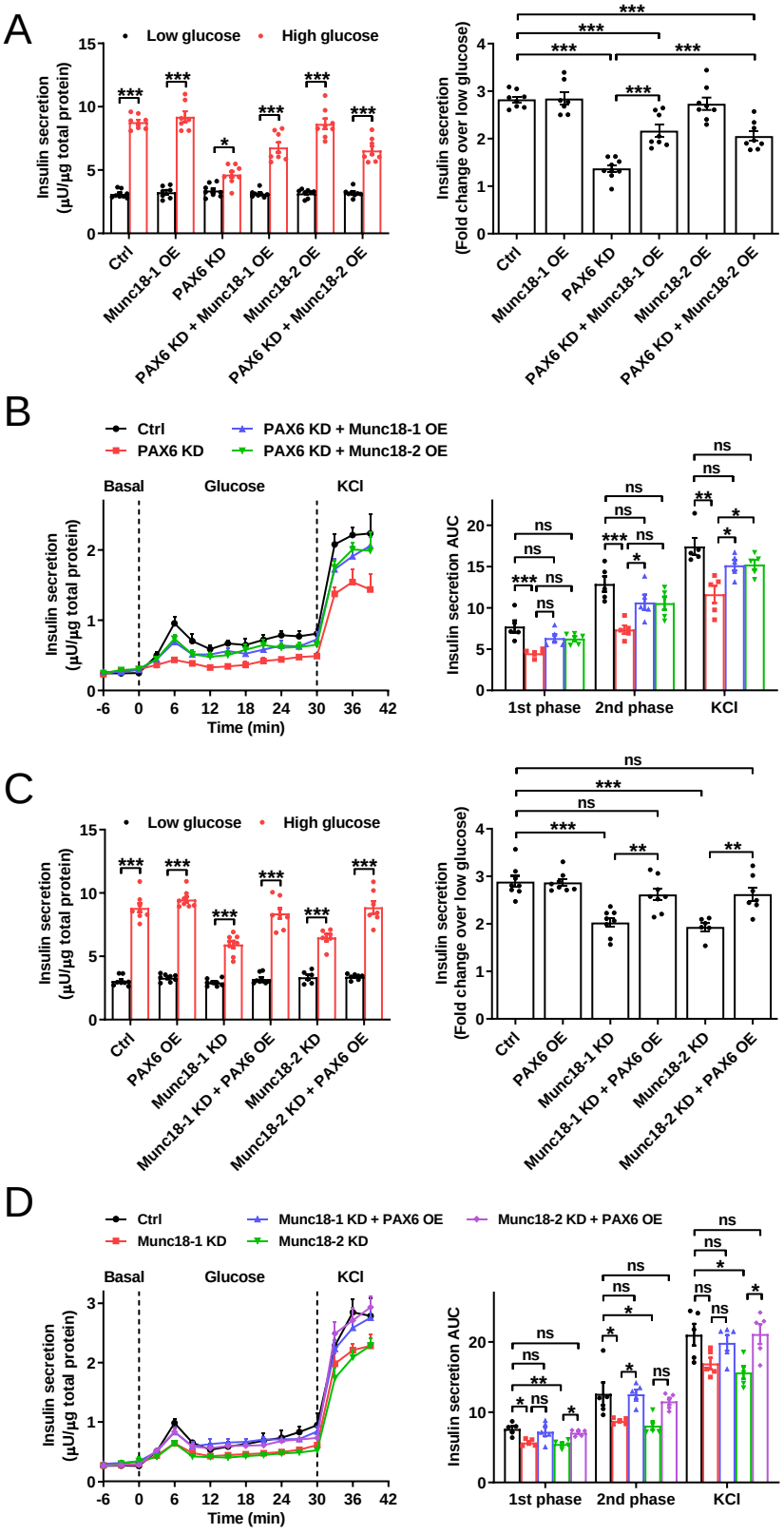
A
Low glucose
High glucose
Insulin secretion (μU/μg total protein)
Ctrl
Munc18-1 OE
PAX6 KD
PAX6 KD + Munc18-1 OE
Munc18-2 OE
PAX6 KD + Munc18-2 OE
Insulin secretion (Fold change over low glucose)
B
Ctrl
PAX6 KD
PAX6 KD + Munc18-1 OE
PAX6 KD + Munc18-2 OE
Basal
Glucose
KCl
Insulin secretion (μU/μg total protein)
Time (min)
Insulin secretion AUC
1st phase
2nd phase
KCl
C
Low glucose
High glucose
Insulin secretion (μU/μg total protein)
Ctrl
PAX6 OE
Munc18-1 KD
Munc18-1 KD + PAX6 OE
Munc18-2 KD
Munc18-2 KD + PAX6 OE
Insulin secretion (Fold change over low glucose)
D
Ctrl
Munc18-1 KD
Munc18-1 KD + PAX6 OE
Munc18-2 KD
Munc18-2 KD + PAX6 OE
Basal
Glucose
KCl
Insulin secretion (μU/μg total protein)
Time (min)
Insulin secretion AUC
1st phase
2nd phase
KCl

Fig. 2. PAX6 regulates GSIS through modulation of Munc18-1/2 expression. (A) Static insulin secretion of EndoC-βH1 cells was expressed as absolute amount (μU/μg total protein) and fold change (*n*=7-9). (B) Dynamic insulin secretion of EndoC-βH1 cells in response to glucose (16.7 mmol/l) and KCl (20 mmol/l) stimulation (*n*=5). (C) Static insulin secretion of EndoC-βH1 cells was expressed as absolute amount (μU/μg total protein) and fold change (*n*=6-8). (D) Dynamic insulin secretion of EndoC-βH1 cells in response to glucose (16.7 mmol/l) and KCl (20 mmol/l) stimulation (*n*=5). **P*<0.05; ***P*<0.01; ****P*<0.001; ns: non-significant. Data are means ± SEMs.

Figure 3

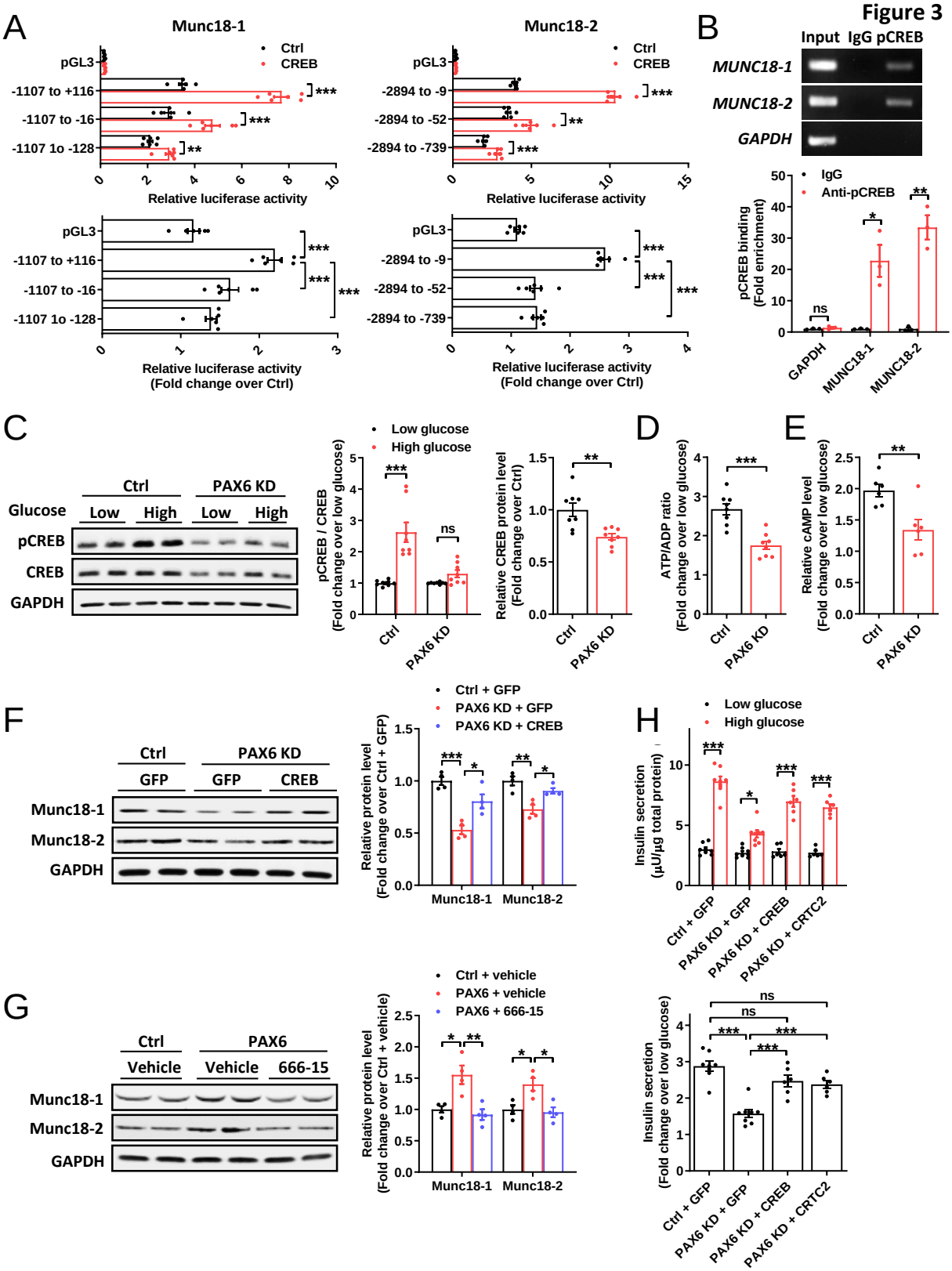
A
Munc18-1
Ctrl
CREB
pGL3
-1107 to +116
-1107 to -16
-1107 1o -128
Relative luciferase activity
Relative luciferase activity
(Fold change over Ctrl)
Munc18-2
-2894 to -9
-2894 to -52
-2894 to -739
B
Input IgG pCREB
MUNC18-1
MUNC18-2
GAPDH
IgG
Anti-pCREB
pCREB binding
(Fold enrichment)
ns
C
Ctrl
PAX6 KD
Glucose
Low
High
pCREB
CREB
GAPDH
Low glucose
High glucose
pCREB / CREB
(Fold change over low glucose)
Relative CREB protein level
(Fold change over Ctrl)
D
ATP/ADP ratio
(Fold change over low glucose)
E
Relative cAMP level
(Fold change over low glucose)
F
GFP
CREB
Munc18-1
Munc18-2
Ctrl + GFP
PAX6 KD + GFP
PAX6 KD + CREB
Relative protein level
(Fold change over Ctrl + GFP)
H
Insulin secretion
(μU/μg total protein)
PAX6 KD + CRTC2
G
Vehicle
666-15
PAX6
Ctrl + vehicle
PAX6 + vehicle
PAX6 + 666-15
Relative protein level
(Fold change over Ctrl + vehicle)
Insulin secretion
(Fold change over low glucose)

Fig. 3. PAX6 regulates Munc18-1/2 expression via modulation of CREB signaling. (A) Luciferase activity of human *MUNC18-1* and *MUNC18-2* promoters was measured in EndoC-βH1 cells (*n*=6). (B) Chromatin immunoprecipitation assay showing pull-down of *MUNC18-1* and *MUNC18-2* promoters by phospho-CREB antibody in EndoC-βH1 cells (*n*=3). (C) Phosphorylated and total CREB levels in EndoC-βH1 cells with PAX6 knockdown after 15-min glucose (2.5 or 20 mmol/l) stimulation (*n*=8). (D) ATP/ADP ratio (*n*=7-8) and (E) cAMP level (*n*=6) were measured in EndoC-βH1 cells with PAX6 knockdown after 15-min glucose (2.5 or 20 mmol/l) stimulation. (F) Protein expression of Munc18-1/2 in EndoC-βH1 cells with PAX6 knockdown and CREB overexpression (*n*=4). (G) Protein expression of Munc18-1/2 in EndoC-βH1 cells with PAX6 overexpression and treatment of CREB inhibitor 666-15 (40 nM) for 72 h (*n*=4). (H) Static insulin secretion of EndoC-βH1 cells was expressed as absolute amount (μU/μg total protein) and fold change (*n*=6). **P*<0.05; ***P*<0.01; ****P*<0.001; ns: non-significant. Data are means ± SEMs.

Figure 4

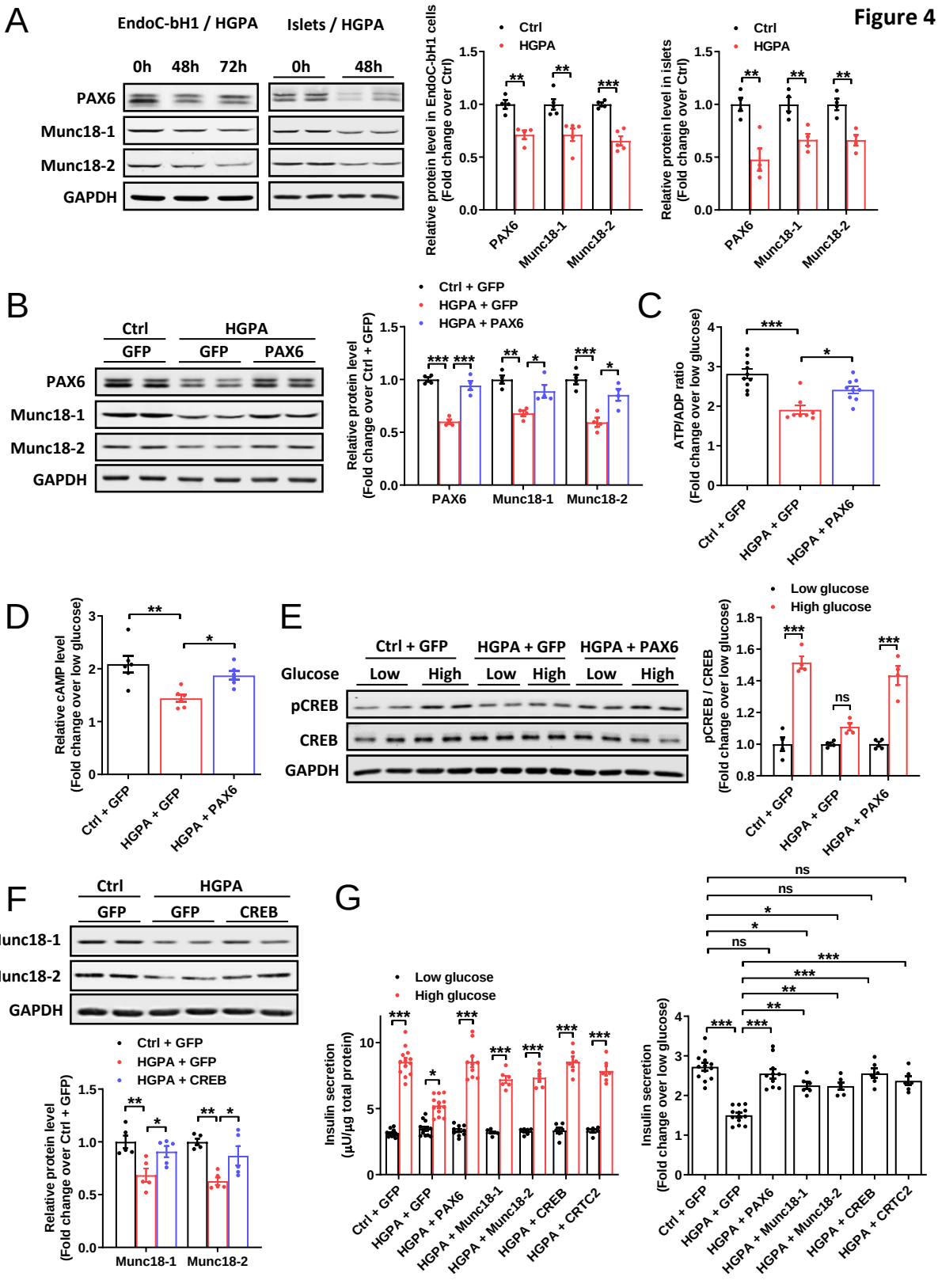
A
EndoC-bH1 / HGPA
Islets / HGPA
0h 48h 72h 0h 48h
PAX6
Munc18-1
Munc18-2
GAPDH
Relative protein level in EndoC-bH1 cells (Fold change over Ctrl)
Ctrl
HGPA
Relative protein level in islets (Fold change over Ctrl)
B
Ctrl
HGPA
GFP GFP PAX6
Ctrl + GFP
HGPA + GFP
HGPA + PAX6
Relative protein level (Fold change over Ctrl + GFP)
C
ATP/ADP ratio (Fold change over low glucose)
D
Relative cAMP level (Fold change over low glucose)
E
Ctrl + GFP
HGPA + GFP
HGPA + PAX6
Glucose
Low High Low High Low High
pCREB
CREB
GAPDH
Low glucose
High glucose
pCREB / CREB (Fold change over low glucose)
ns
F
Ctrl
HGPA
GFP GFP CREB
Munc18-1
Munc18-2
GAPDH
Ctrl + GFP
HGPA + GFP
HGPA + CREB
Relative protein level (Fold change over Ctrl + GFP)
G
Low glucose
High glucose
Insulin secretion (μU/μg total protein)
Ctrl + GFP
HGPA + GFP
HGPA + PAX6
HGPA + Munc18-1
HGPA + Munc18-2
HGPA + CREB
HGPA + CRTC2
Insulin secretion (Fold change over low glucose)

Fig. 4. Repressed PAX6/CREB/Munc18 axis in pancreatic beta-cells under diabetic condition leads to blunted insulin secretion. (A) Protein expression of PAX6 and Munc18-1/2 in EndoC-βH1 cells and isolated mouse islets exposed to HGPA for the indicated periods of time (*n*=4-5). (B) Protein expression of PAX6 and Munc18-1/2 in EndoC-βH1 cells with PAX6 overexpression after 72-h exposure to normal or HGPA condition (*n*=4). After 72-h exposure to normal or HGPA condition, (C) ATP/ADP ratio (*n*=8-10), (D) cAMP level (*n*=6), (E) phosphorylated and total CREB levels (*n*=4) in EndoC-βH1 cells with PAX6 overexpression were measured after 15-min glucose (2.5 or 20 mmol/l) stimulation. (F) Protein expression of Munc18-1/2 in EndoC-βH1 cells with CREB overexpression after 72-h exposure to normal or HGPA condition (*n*=5). (G) Static insulin secretion of EndoC-βH1 cells was expressed as absolute amount (μU/μg total protein) and fold change (*n*=6-11). **P*<0.05; ***P*<0.01; ****P*<0.001; ns: non-significant. Data are means ± SEMs.

Figure 5

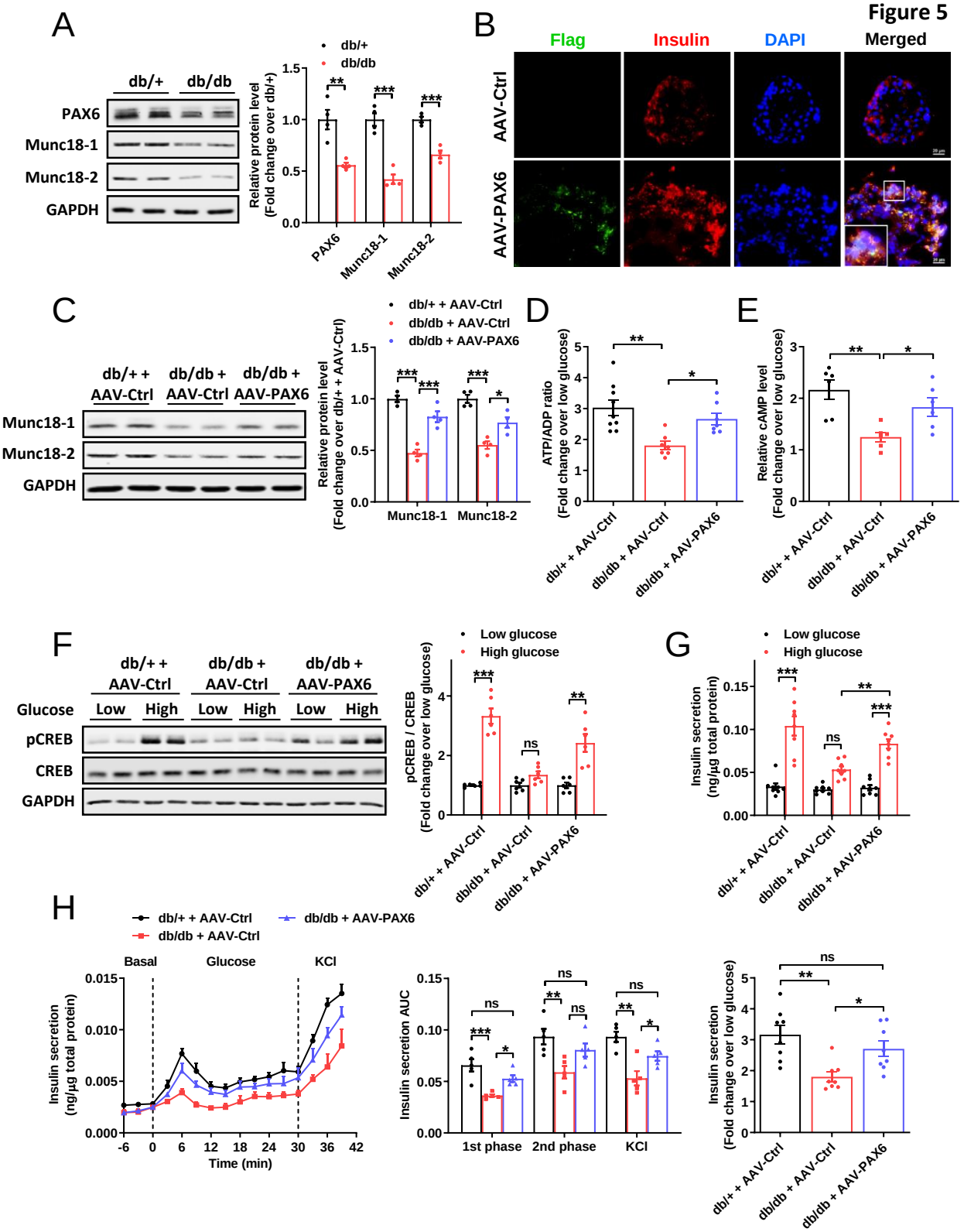
A
db/+
db/db
PAX6
Munc18-1
Munc18-2
GAPDH
Relative protein level (Fold change over db/+)
B
Flag
Insulin
DAPI
Merged
AAV-Ctrl
AAV-PAX6
C
db/+ + AAV-Ctrl
db/db + AAV-Ctrl
db/db + AAV-PAX6
Relative protein level (Fold change over db/+ + AAV-Ctrl)
D
ATP/ADP ratio (Fold change over low glucose)
E
Relative cAMP level (Fold change over low glucose)
F
Glucose
Low
High
pCREB
CREB
pCREB / CREB (Fold change over low glucose)
G
Insulin secretion (ng/μg total protein)
H
Basal
Glucose
KCl
Time (min)
Insulin secretion AUC
1st phase
2nd phase
KCl

1

2

Fig. 5. Beta-cell specific PAX6 overexpression preserves CREB/Munc18-1/2 signaling pathway and GSIS in *db/db* mouse islets. (A) Protein expression of PAX6 and Munc18-1/2 in isolated islets of *db/+* and *db/db* mice (n=4). (B) Representative immunostaining of *db/db* mouse islets labeled for flag (green), insulin (red) and DAPI (blue) 6-week post AAV injection. Scale bar = 20 μm. (C) Protein expression of Munc18-1/2 in isolated islets of *db/+* and *db/db* mice with AAV-Ctrl or AAV-PAX6 injection (n=4). (D) ATP/ADP ratio (n=7-9) and (E) cAMP level (n=6) in dispersed mouse islet cells after 15-min glucose (2.5 or 20 mmol/l) stimulation. (F) Phosphorylated and total CREB levels in isolated islets of *db/+* and *db/db* mice after 15-min glucose (2.5 or 20 mmol/l) stimulation (n=4). (G) Static insulin secretion of isolated islets of *db/+* and *db/db* mice was expressed as absolute amount (ng/μg total protein) and fold change (n=8). (H) Dynamic insulin secretion of isolated islets in response to glucose (16.7 mmol/l) and KCl (20 mmol/l) stimulation (n=5). **P*<0.05; ***P*<0.01; ****P*<0.001; ns: non-significant. Data are means ± SEMs.

Figure 6

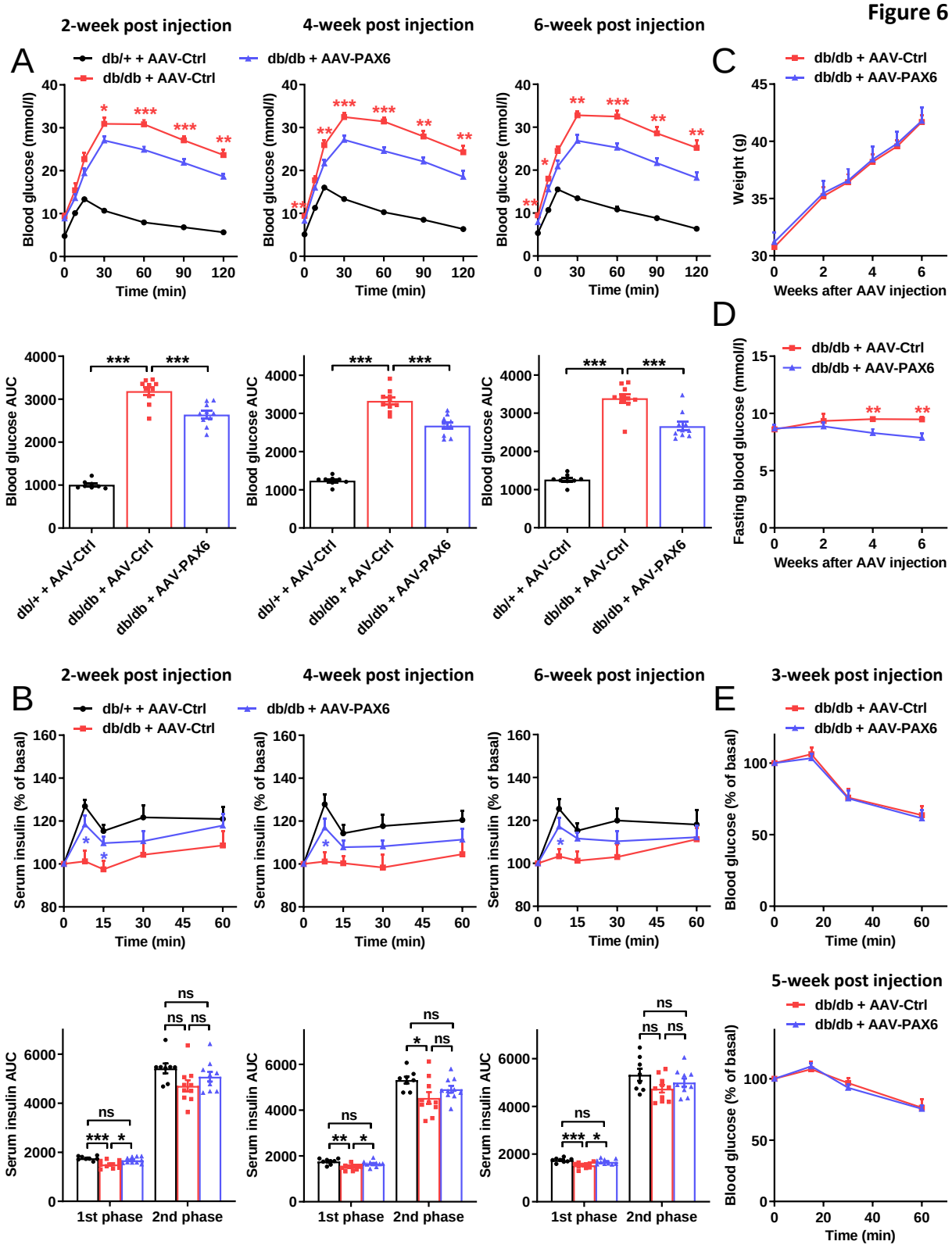
A
2-week post injection
4-week post injection
6-week post injection
db/+ + AAV-Ctrl
db/db + AAV-Ctrl
db/db + AAV-PAX6
Blood glucose (mmol/l)
Time (min)
Blood glucose AUC
C
Weight (g)
Weeks after AAV injection
D
Fasting blood glucose (mmol/l)
B
Serum insulin (% of basal)
Serum insulin AUC
1st phase
2nd phase
E
3-week post injection
5-week post injection
Blood glucose (% of basal)
ns

1

2

Fig. 6. Beta-cell specific PAX6 overexpression improves glucose homeostasis in *db/db* mice. (A) Glucose tolerance by IPGTT was performed 2-, 4- and 6-week post AAV injection with glucose profiles calculated as AUC. **P*<0.05; ***P*<0.01; ****P*<0.001 versus *db/db* + AAV-PAX6. (B) Serum insulin levels during IPGTT were expressed as % of basal. **P*<0.05 versus *db/db* + AAV-Ctrl. (C) Weight and (D) fasting blood glucose at the indicated time points after AAV injection. (E) ITT was performed 3- and 5-week post AAV injection and blood glucose levels were expressed as % of basal level. **P*<0.05; ***P*<0.01; ****P*<0.001; ns: non-significant (*n*=8-10). Data are means ± SEMs.

Figure 7

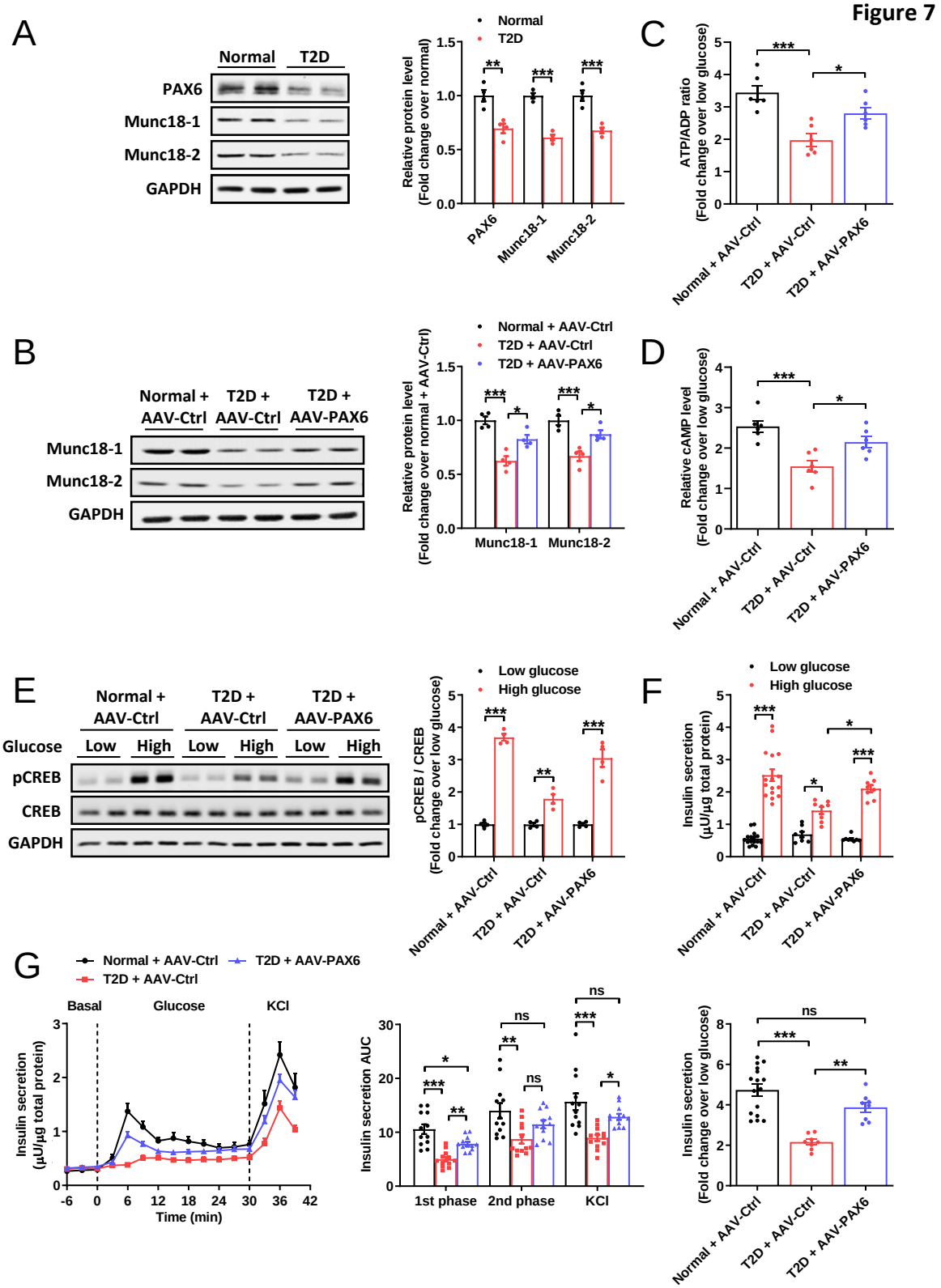
A
Normal
T2D
PAX6
Munc18-1
Munc18-2
GAPDH
Relative protein level (Fold change over normal)
C
ATP/ADP ratio (Fold change over low glucose)
Normal + AAV-Ctrl
T2D + AAV-Ctrl
T2D + AAV-PAX6
B
Normal + AAV-Ctrl
T2D + AAV-Ctrl
T2D + AAV-PAX6
Munc18-1
Munc18-2
GAPDH
Relative protein level (Fold change over normal + AAV-Ctrl)
D
Relative cAMP level (Fold change over low glucose)
E
Glucose
Low
High
pCREB
CREB
GAPDH
pCREB / CREB (Fold change over low glucose)
Low glucose
High glucose
F
Insulin secretion (μU/μg total protein)
G
Basal
Glucose
KCl
Time (min)
Insulin secretion AUC
1st phase
2nd phase
KCl
ns

1

2

Fig. 7. Beta-cell specific PAX6 overexpression restores CREB/Munc18-1/2 signaling pathway and GSIS in T2D human islets. (A) Protein expression of PAX6 and Munc18-1/2 in normal and T2D human islets (*n*=4). (B) Protein expression of Munc18-1/2 in human islets with AAV-Ctrl or AAV-PAX6 transduction (*n*=4). (C) ATP/ADP ratio (*n*=6) and (D) cAMP level (*n*=6) in dispersed human islet cells after 15-min glucose (2.5 or 20 mmol/l) stimulation. (E) Phosphorylated and total CREB levels in human islets after 15-min glucose (2.5 or 20 mmol/l) stimulation (*n*=4). (F) Static insulin secretion of human islets was expressed as absolute amount (μU/μg total protein) and fold change (*n*=8-16). (G) Dynamic insulin secretion of human islets in response to glucose (16.7 mmol/l) and KCl (20 mmol/l) stimulation (*n*=12). **P*<0.05; ***P*<0.01; ****P*<0.001; ns: non-significant. Data are means ± SEMs.

Supplementary Materials

Figure S1

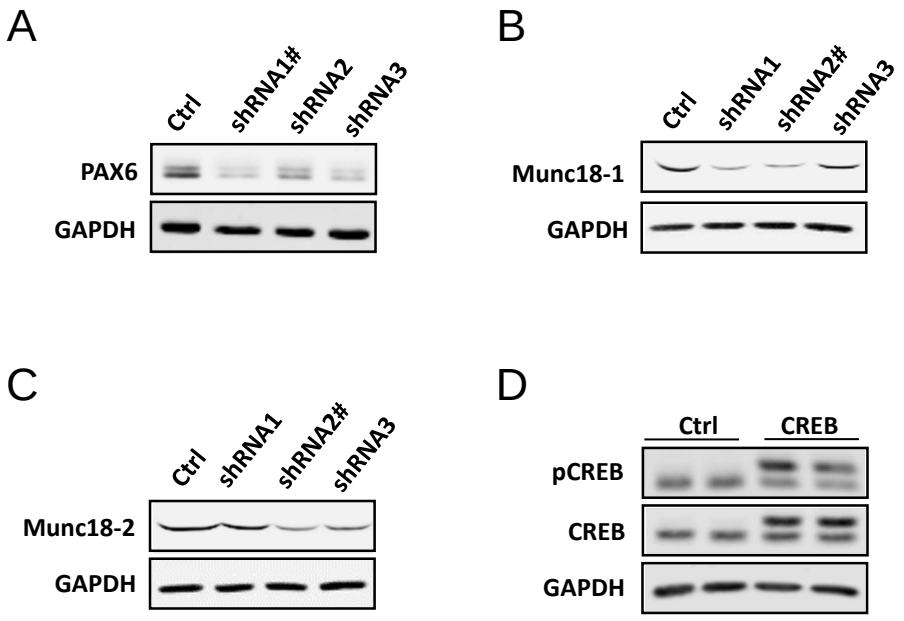

Fig. S1. Western blotting showing knockdown efficiency of three shRNA constructs targeting human (A) PAX6, (B) Munc18-1 and (C) Munc18-2 in EndoC-βH1 cells. Hashtags indicate the shRNA constructs chosen for downstream experiments. (D) Western blotting showing the increase in phosphorylated and total CREB in EndoC-βH1 cells with CREB overexpression.

Figure S2

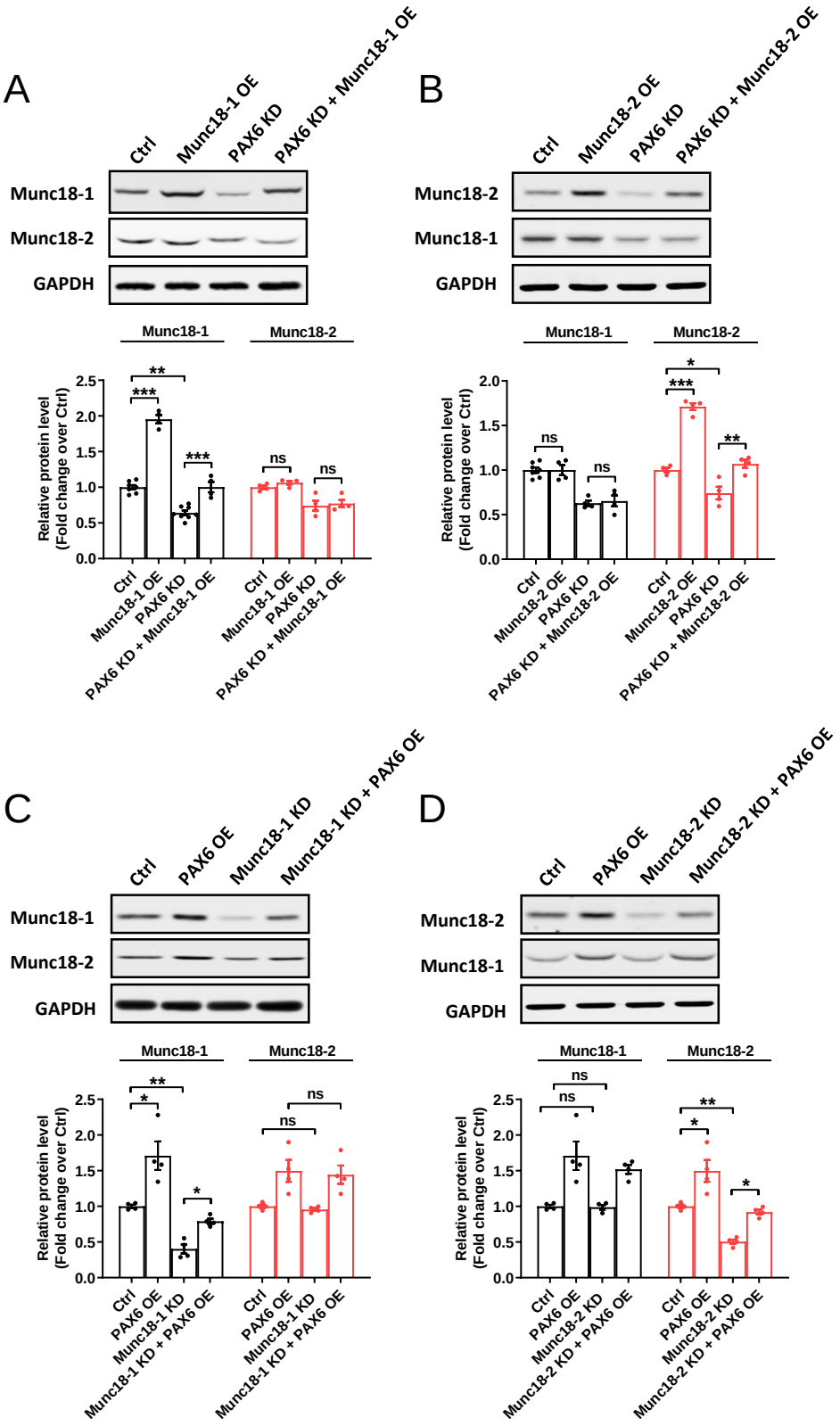
A
Ctrl
Munc18-1 OE
PAX6 KD
PAX6 KD + Munc18-1 OE
Munc18-1
Munc18-2
GAPDH
Munc18-1
Munc18-2
Relative protein level (Fold change over Ctrl)
Ctrl
Munc18-1 OE
PAX6 KD
PAX6 KD + Munc18-1 OE
B
Ctrl
Munc18-2 OE
PAX6 KD
PAX6 KD + Munc18-2 OE
Munc18-2
Munc18-1
GAPDH
Munc18-1
Munc18-2
Relative protein level (Fold change over Ctrl)
Ctrl
Munc18-2 OE
PAX6 KD
PAX6 KD + Munc18-2 OE
C
Ctrl
PAX6 OE
Munc18-1 KD
Munc18-1 KD + PAX6 OE
Munc18-1
Munc18-2
GAPDH
Munc18-1
Munc18-2
Relative protein level (Fold change over Ctrl)
Ctrl
PAX6 OE
Munc18-1 KD
Munc18-1 KD + PAX6 OE
D
Ctrl
PAX6 OE
Munc18-2 KD
Munc18-2 KD + PAX6 OE
Munc18-2
Munc18-1
GAPDH
Munc18-1
Munc18-2
Relative protein level (Fold change over Ctrl)
Ctrl
PAX6 OE
Munc18-2 KD
Munc18-2 KD + PAX6 OE

Fig. S2. Western blotting showing Munc18-1/2 expression in EndoC-βH1 cells under different conditions: (A) cells with Munc18-1 overexpression, PAX6 knockdown and PAX6 knockdown with Munc18-1 overexpression; (B) cells with Munc18-2 overexpression, PAX6 knockdown and PAX6 knockdown with Munc18-2 overexpression; (C) cells with PAX6 overexpression, Munc18-1 knockdown and Munc18-1 knockdown with PAX6 overexpression; (D) cells with PAX6 overexpression, Munc18-2 knockdown and Munc18-2 knockdown with PAX6 overexpression (n=4-8). *P<0.05; **P<0.01; ***P<0.001; ns: non-significant. Data are means ± SEMs.

Figure S3

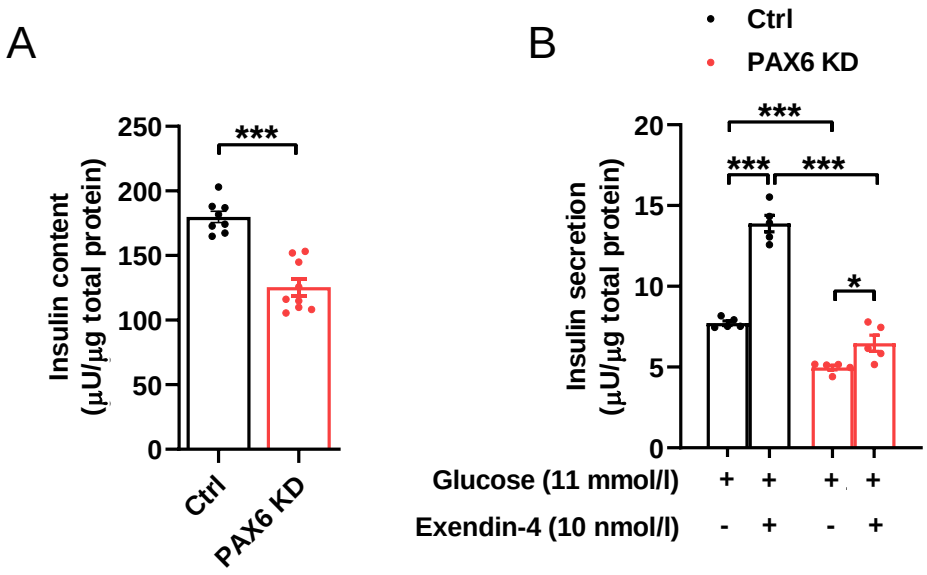

Fig. S3. Effects of PAX6 knockdown on insulin content and insulin secretion in EndoC-βH1 cells. (A) Insulin content was expressed as absolute amount (µU/µg total protein) (*n*=8-9). (B) Control or PAX6 knockdown cells were stimulated with exendin-4 (10 nmol/l) in the presence of 11 mmol/l glucose for 1 h. Insulin secretion was expressed as absolute amount (µU/µg total protein) (*n*=5). **P*<0.05; ****P*<0.001. Data are means ± SEMs.

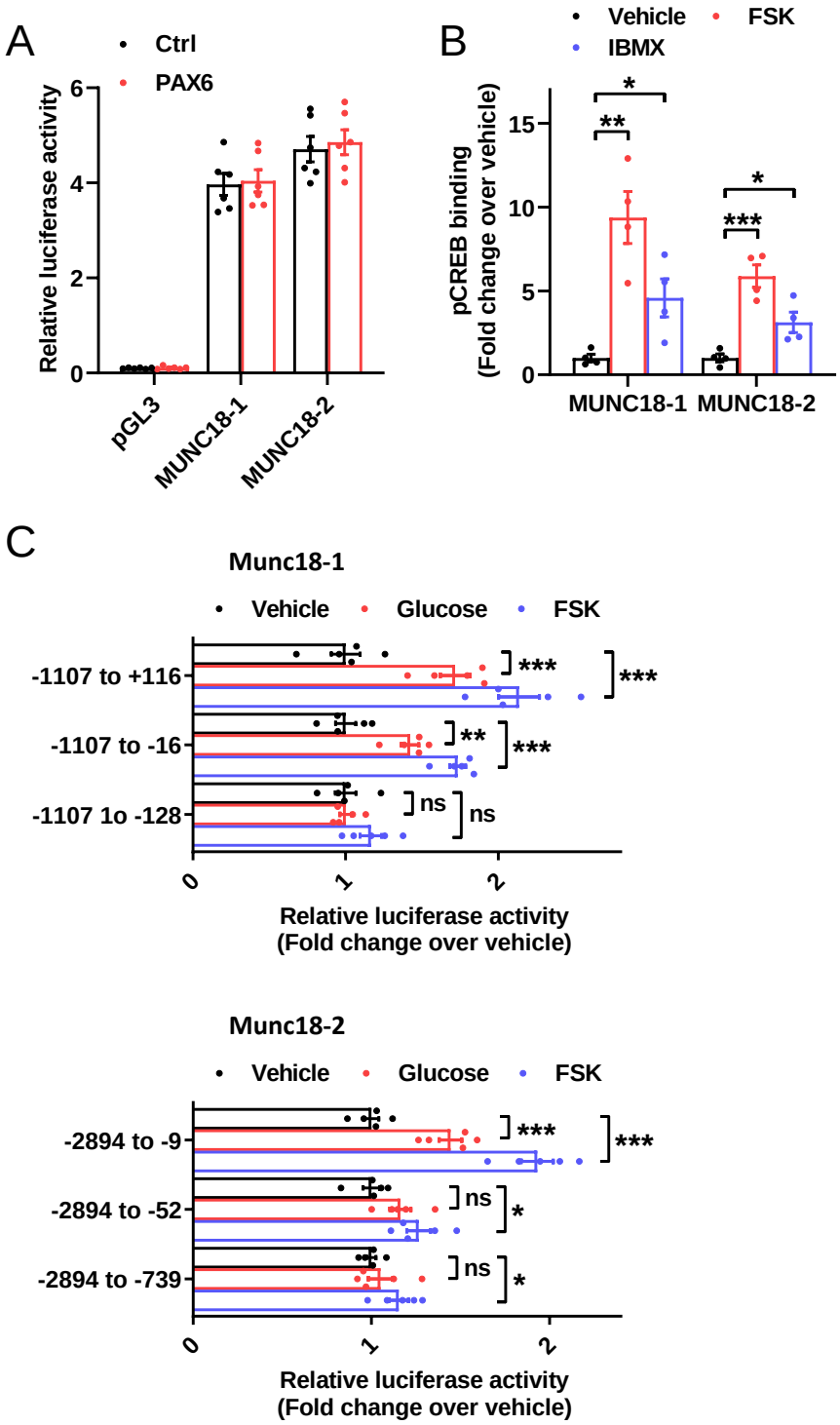

Fig. S4. (A) Luciferase activity of human *MUNC18-1* and *MUNC18-2* promoters was measured in EndoC-βH1 cells with or without PAX6 overexpression (*n*=6). (B) Chromatin

immunoprecipitation assay showing increased pCREB binding onto *MUNC18-1* and *MUNC18-2* promoters after 2 h treatment of FSK (10 μmol/l) or IBMX (300 μmol/l) in EndoC-βH1 cells (n=4). (C) Luciferase reporter assay showing enhanced activity of human *MUNC18-1* and *MUNC18-2* promoters after 16 h treatment of glucose (20 mmol/l) or FSK (10 μmol/l) in EndoC-βH1 cells (n=5). *P<0.05; **P<0.01; ***P<0.001; ns: non-significant. Data are means ± SEMs.

Figure S5

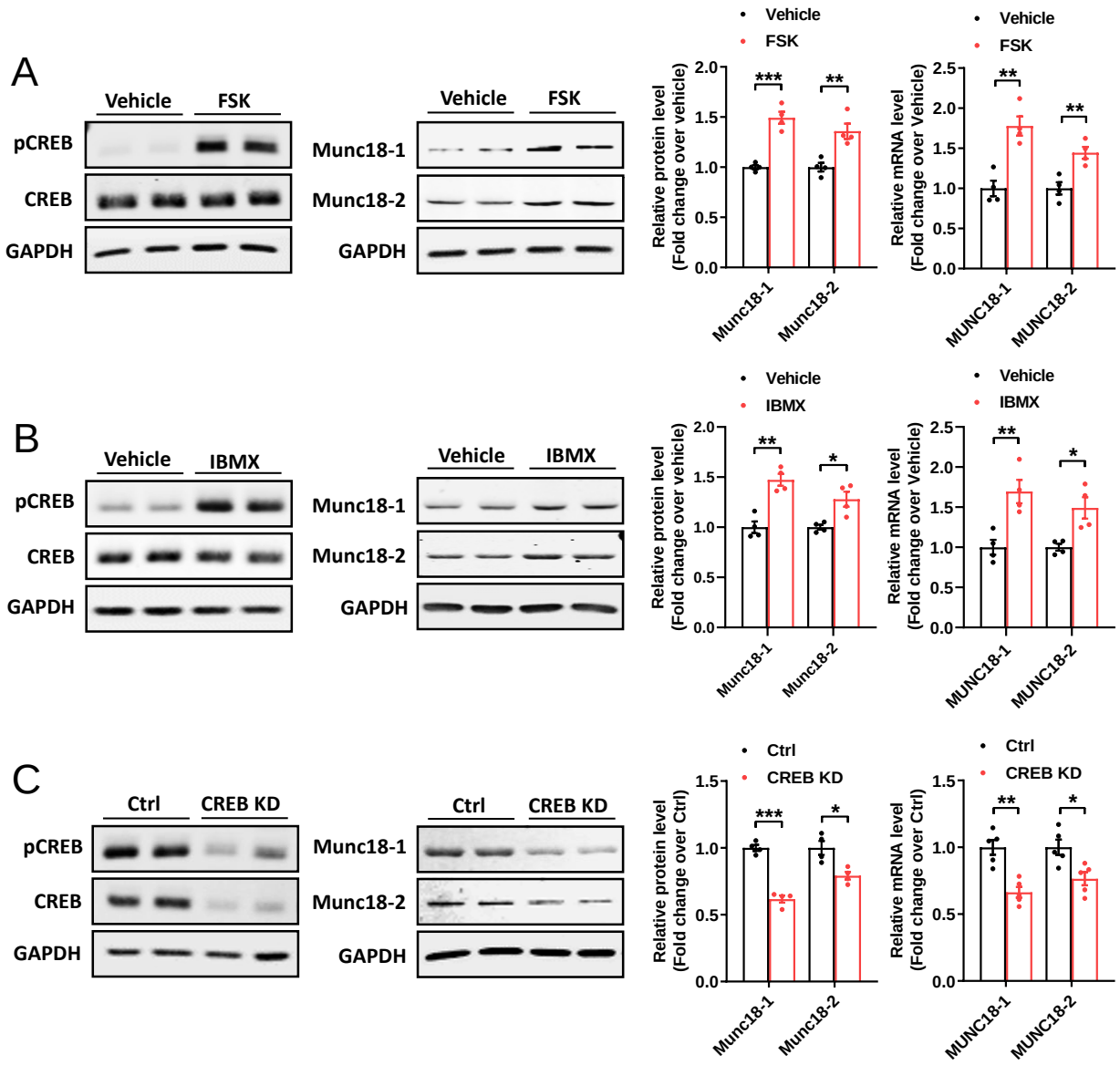

Fig. S5. Phosphorylation of CREB, Munc18-1 and Munc18-2 protein and mRNA levels in EndoC-βH1 cells after 24-h treatment of (A) FSK (10 μmol/l) or (B) IBMX (300 μmol/l) (*n*=4). (C) Phosphorylation of CREB, Munc18-1 and Munc18-2 protein and mRNA levels in control and CREB knockdown cells (*n*=4-5). **P*<0.05; ***P*<0.01; ****P*<0.001. Data are means ± SEMs.

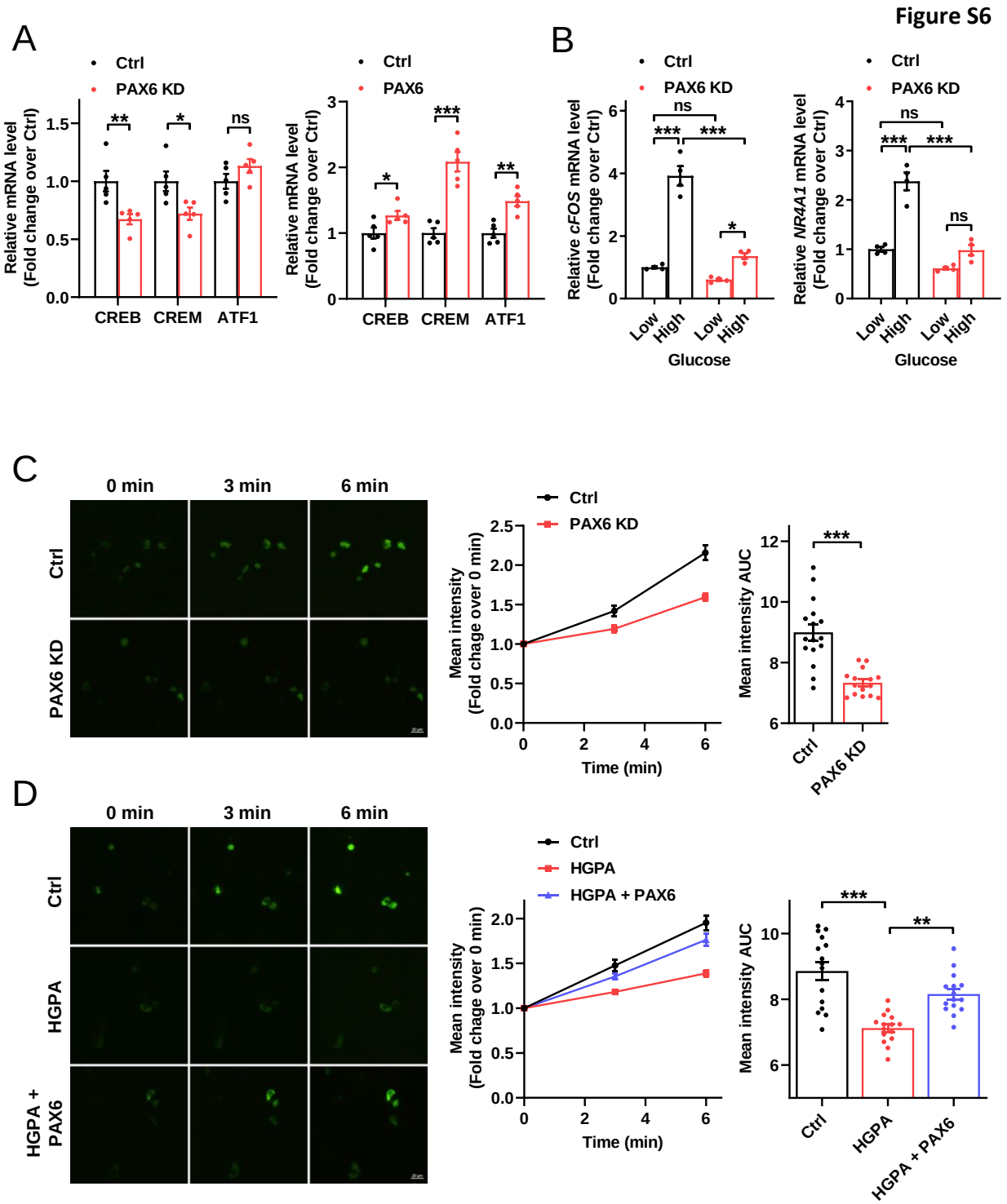

Fig. S6. (A) mRNA levels of *CREB*, *CREM* and *ATF1* in EndoC-βH1 cells with PAX6 knockdown and overexpression (n=5). (B) Attenuated glucose-induced expression of *cFOS* and

NR4A1 mRNA levels in PAX6 knockdown cells. EndoC-βH1 cells were stimulated with low (2.5 mmol/l) or high (20 mmol/l) glucose for 1 h (n=4). Measurement of Ca^{2+} influx by live-cell imaging of EndoC-βH1 cells under (C) control and PAX6 knockdown conditions and under (D) control and HGPA conditions with or without PAX6 overexpression. Representative images of cells after 3- and 6-min glucose (20 mmol/l) stimulation are shown. Scale bar = 20 μm. *P<0.05; **P<0.01; ***P<0.001; ns: non-significant. Data are means ± SEMs.

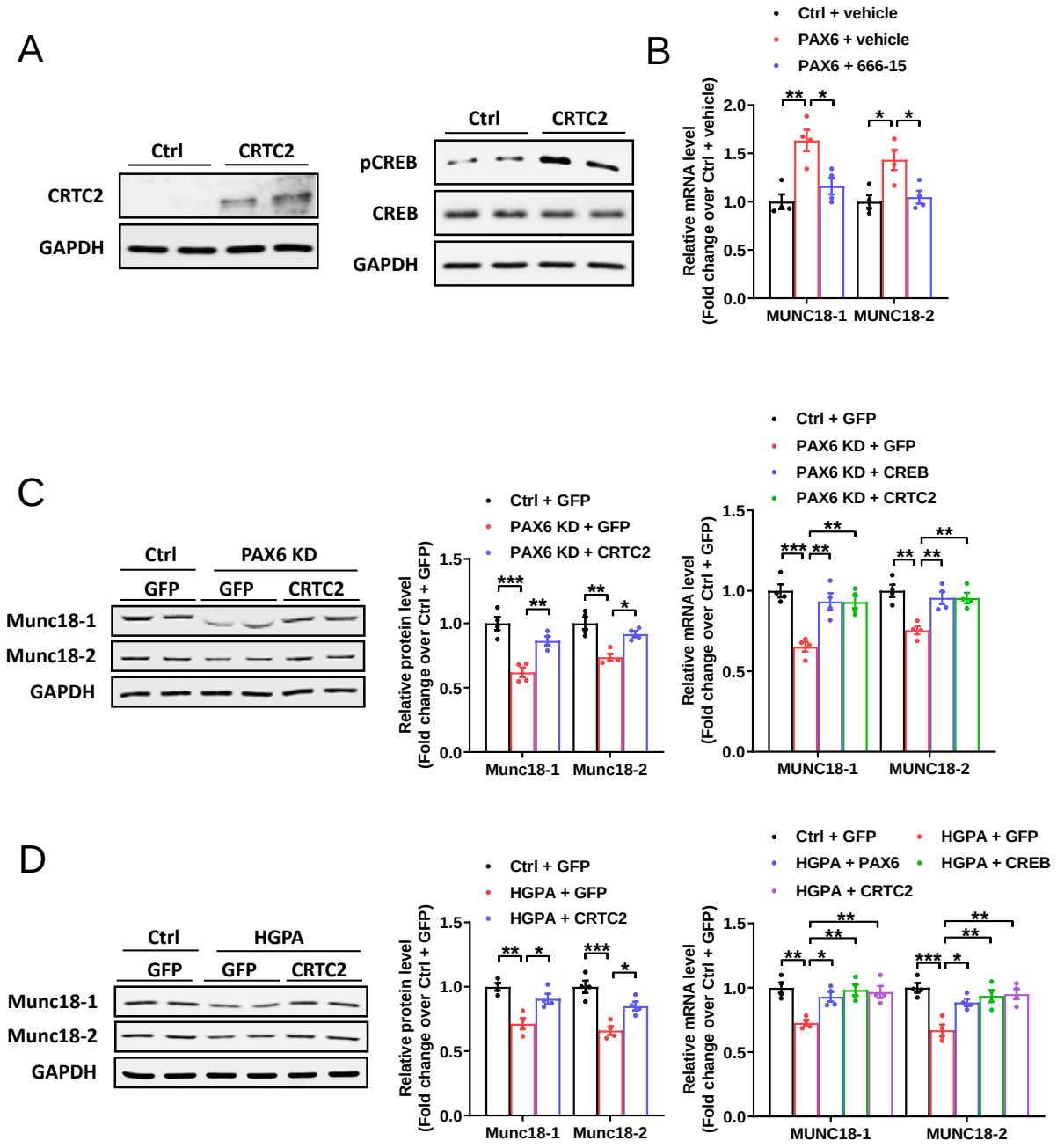

Fig. S7. (A) Western blotting showing overexpression of CRTC2 and increased phosphorylated CREB in EndoC-βH1 cells. (B) mRNA levels of *MUNC18-1* and *MUNC18-2* in EndoC-βH1

cells with PAX6 overexpression and treatment of CREB inhibitor 666-15 (40 nM) for 72 h (n=4). (C) Protein and mRNA expression of Munc18-1/2 in EndoC-βH1 cells with PAX6 knockdown and CREB/ CRTC2 overexpression (n=4). (D) Protein and mRNA expression of Munc18-1/2 in EndoC-βH1 cells with CREB/ CRTC2 overexpression after 72-h exposure to normal or HGPA condition (n=4). *P<0.05; **P<0.01; ***P<0.001. Data are means ± SEMs.

Figure S8

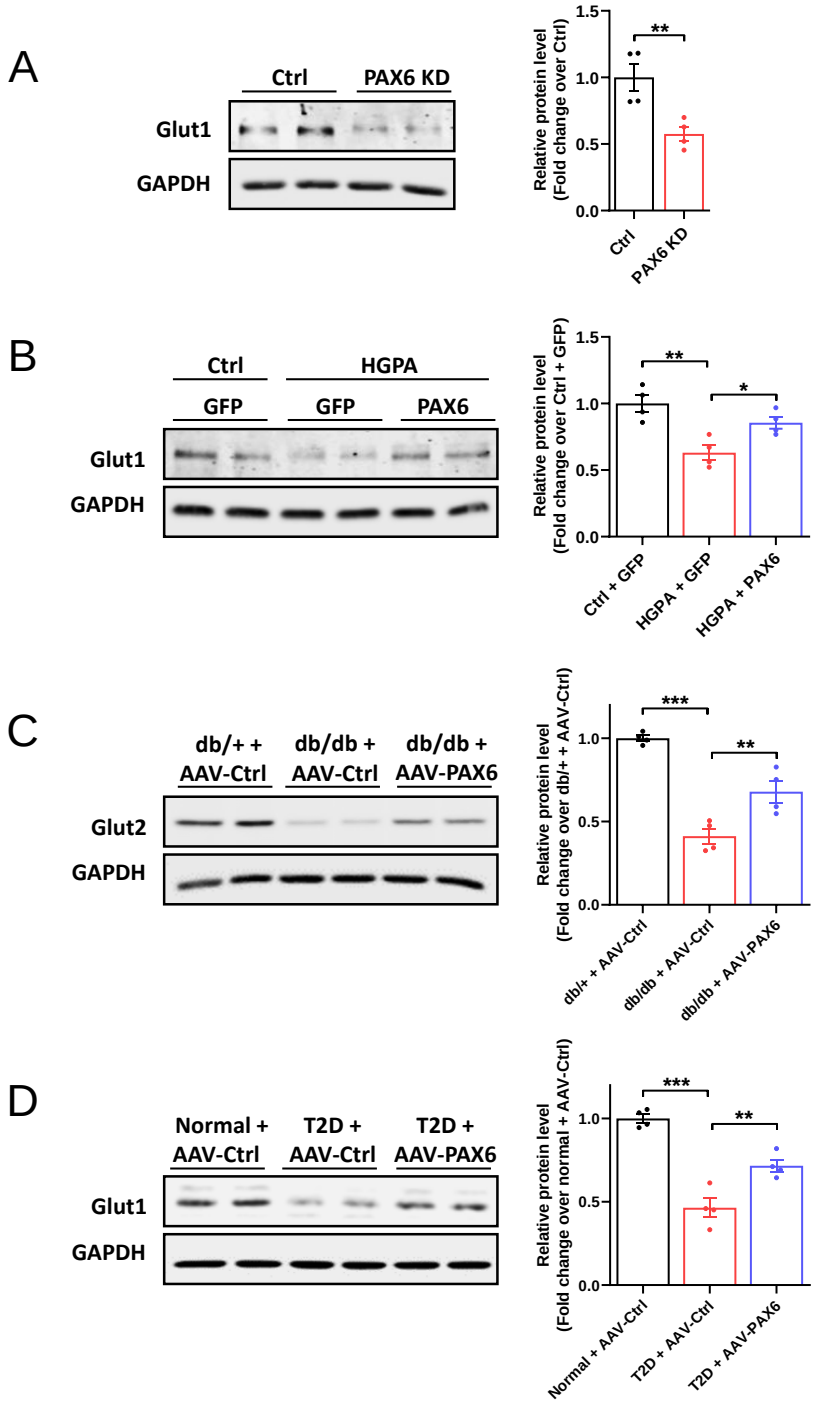

Fig. S8. Western blotting showing Glut1 and Glut2 protein expression. (A) Protein expression of Glut1 in EndoC-βH1 cells with PAX6 knockdown. (B) Protein expression of Glut1 in EndoC-

βH1 cells with PAX6 overexpression after 72-h exposure to normal or HGPA condition. (C) Protein expression of Glut2 in isolated islets of *db/+* and *db/db* mice 6-week post AAV-Ctrl or AAV-PAX6 injection. (D) Protein expression of Glut1 in human islets with AAV-Ctrl or AAV-PAX6 transduction (n=4). *P<0.05; **P<0.01; ***P<0.001. Data are means ± SEMs.

Mouse islets

Figure S9

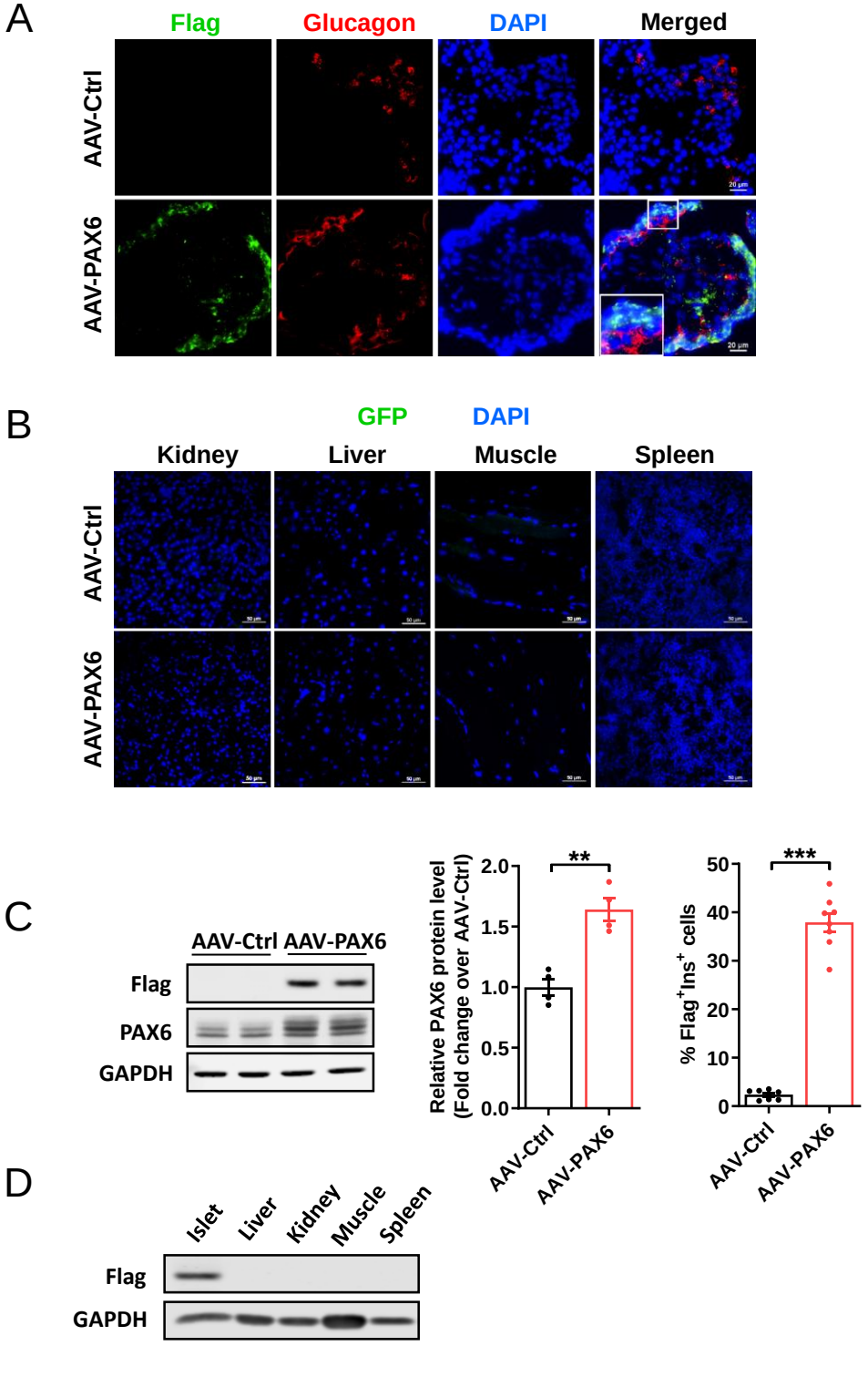

1

2

Fig. S9. (A) Representative immunostaining of *db/db* mouse islets labeled for flag (green), glucagon (red) and DAPI (blue). Scale bar = 20 μm. (B) Representative immunostaining of *db/db* mouse kidney, liver, muscle and spleen labeled for GFP (green) and DAPI (blue). Scale bar = 50 μm. Tissues were harvested in *db/db* mice 6-week post AAV injection. (C) Western blotting and quantification showing the expression of exogenous PAX6 in *db/db* mouse islets with AAV-PAX6 injection. (D) Western blotting showing the absence of flag tag in other *db/db* mouse organs. $^{**}P<0.01$; $^{***}P<0.001$. Data are means ± SEMs.

Figure S10

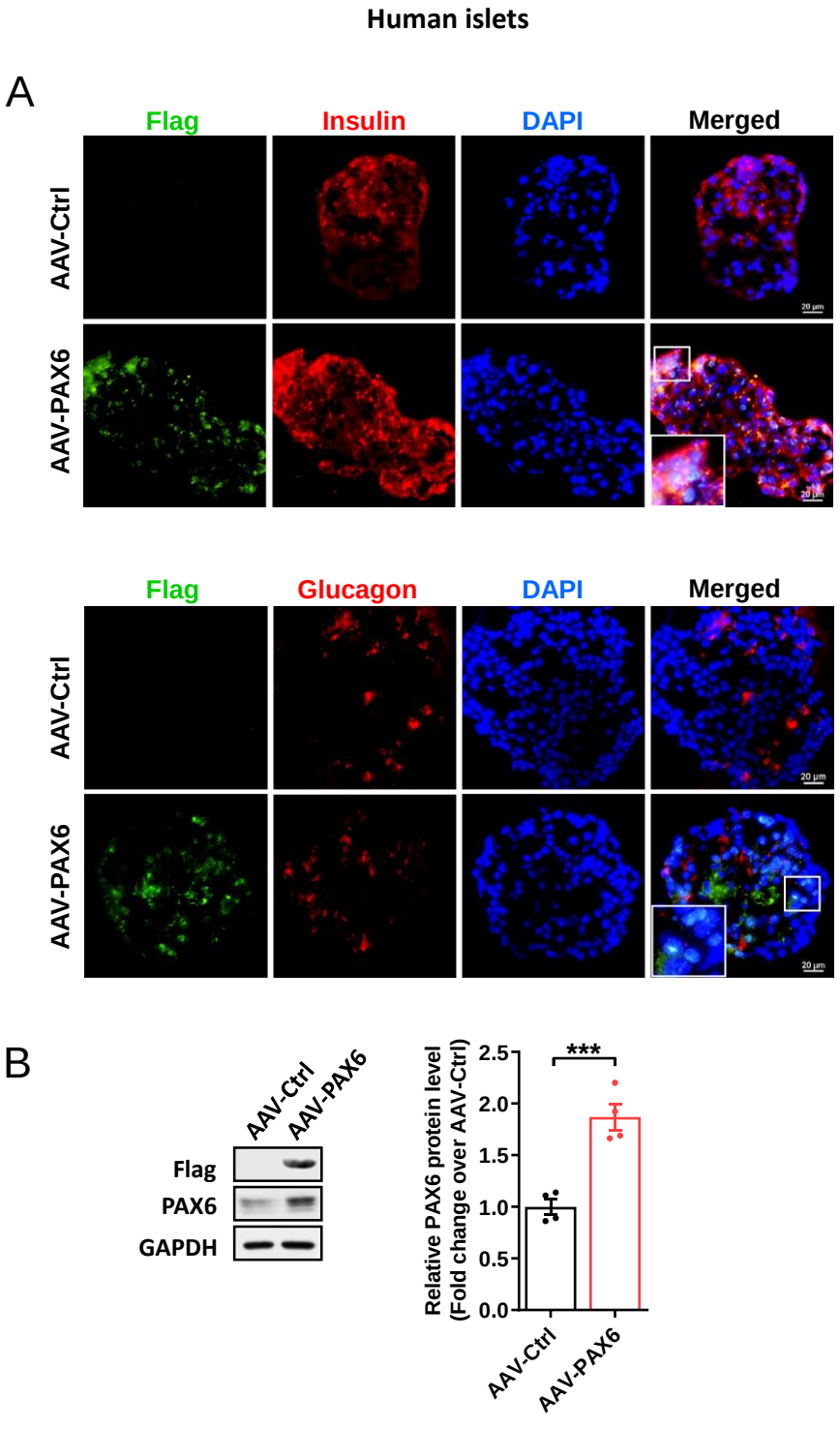

Fig. S10. (A) Representative immunostaining of human T2D islets labeled for flag (green), insulin or glucagon (red) and DAPI (blue) with AAV transduction. Scale bar = 20 μm. (B)

Western blotting and quantification showing the expression of exogenous PAX6 in T2D islets with AAV-PAX6 transduction. ***P<0.001. Data are means ± SEMs.

Table S1

shRNA for gene knockdown	shRNA sequence
PAX6	AATTCTGGGCAGGTATTACGA
MUNC18-1	TATGATCTGCTGCCTATCGAA
MUNC18-2	ATATCTTCTTCACCGACACCT
CREB1	ACAGCACCCACTAGCACTATT
Non-targeting control	CAACAAGATGAAGAGCACCAA

Primers for qPCR	Forward primer (5'-3')	Reverse primer (5'-3')
b-actin	ACAGAGCCTCGCCTTTGCC	GATATCATCATCCATGGTGAGCTGG
PAX6	AACGATAACATACCAAGCGTGT	GGTCTGCCCGTTCAACATC
MUNC18-1	AAAGCTGTTGTCGGAGAGAAG	CACAATCGTTATGCCCTCGG
MUNC18-2	ATTCTGAGCGGAGTTATTCGGA	CCGCCGTTTGTTGATGTCTTC
MUNC18-3	AGCAACAGTGTTTGATGACTGC	TCTGACAGGTTCACGGTTCTTA
MUNC13-1	CGATGATCGGGAACCTCTTG	AGCTCCTTGGCTGCATTGAA
SNAP25	ATGGATGAAAACCTAGAGCAGG	ACACTTAACCACTTCCCAGC
SYB2	CTCAAGCGCAAATACTGGTGG	TGATGGCGCAAATCACTCCC
STX1A	TAAAGAGCATCGAGCAGTCCA	GACATGACCTCCACAAACTTTCT
cFOS	GGGGCAAGGTGGAACAGTTAT	AGGTTGGCAATCTCGGTCTG
NR4A1	AGGGCTGCAAGGGCTTCT	GGCAGATGTACTTGGCGTTTTT
CREB1	GTGACGGAGGAGCTTGTACC	GCTGCTGGCATAGATACCTGG
CREM	ACAATGAGCAAATGTGCAAGGA	TCTGCAATTGCTGCTACCTGA
ATF1	GGTAGCTTAGGACAGTTGGC	CTGATAAAGATGATACCTGTTGAGC

Primers for luciferase vectors construction	Forward primer (5'-3')	Reverse primer (5'-3')
MUNC18-1 (-1107 to +116)	ACTGACGCTAGCCTCCTATTAACAAAGAAA	ACTGACAAGCTTGGCGCTGCGCGAGTCTCC
MUNC18-1 (-1107 to -16)	ACTGACGCTAGCCTCCTATTAACAAAGAAA	ACTGACAAGCTTCGCGGACTGGGCGCGGGG
MUNC18-1 (-1107 to -128)	ACTGACGCTAGCCTCCTATTAACAAAGAAA	ACTGACAAGCTTCCCACTCGCCTCCGCCAA
MUNC18-2 (-2894 to -9)	ACTGACGCTAGCCACTGTGGCTTTCCCTCA	ACTGACAAGCTTCTTCCGGGTGTGTCCCAA
MUNC18-2 (-2894 to -52)	ACTGACGCTAGCCACTGTGGCTTTCCCTCA	ACTGACAAGCTTCCCACGTGGACCCCGCCC
MUNC18-2 (-2894 to -739)	ACTGACGCTAGCCACTGTGGCTTTCCCTCA	ACTGACAAGCTTCCCTCAAATGCTTGCAAA

Primers for ChIP assay	Forward primer (5'-3')	Reverse primer (5'-3')
MUNC18-1	GGGTTTCAGGCAGATGGA	TACCCAGGCCTCCTCTTTC
MUNC18-2	CTCCCATCTGTGAGCGTGT	AGGCCCAGGAAGTTGAGTC
GAPDH	TTGACTCACCCTGCCCTCAAT	CCTCCCACAAAGGCACTCCT

Table S1. Oligonucleotide sequences used in shRNA vectors construction, qPCR, luciferase vectors construction and ChIP assay.

Table S2

Species	Gene	Position	Sequence
Human	*MUNC18-1*	-127 to -120	TGACGCCA
		-15 to -11	CGTCA
	MUNC18-2	-738 to -734	CGTCA
		-51 to -44	TGACGCGC
Mouse	*Munc18-1*	-195 to -191	TGACG
		-189 to -185	TGACG
		-83 to -79	CGTCA
	Munc18-2	-1296 to -1292	CGTCA
		-45 to -38	TGACGCGT

Table S2. Sequences and positions of putative CREs in promoters of Munc18-1 and Munc18-2 in both human and mouse.

Table S3

Donor ID	Age	Gender	Weight (lbs)	BMI	HbA1c (%)
Normal 1	23	F	157	24.5	4.9
Normal 2	41	M	218	35.12	5.8
Normal 3	51	M	195	31.45	5.2
Normal 4	55	M	160	23.63	4.7
T2D 1	55	F	164	29.9	7.4
T2D 2	63	M	234	31.69	6.9
T2D 3	52	M	158	24.75	7.6
T2D 4	59	M	168	25.54	7.3

Table S3. Human islet donor information.